# Fragmentation of polypropylene into microplastics promoted by photo-aging; release of metals, toxicity and inhibition of biodegradability

Josipa Papac Zjacić, Zvonimir Katančić, Marin Kovacic, Hrvoje Kusic, Zlata Hrnjak Murgić, Dionysios D Dionysiou, Panaghiotis Karamanis, Ana Loncaric Bozic


# Fragmentation of polypropylene into microplastics promoted by photo-aging; release of metals, toxicity and inhibition of biodegradability

Josipa Papac Zjačić, Zvonimir Katančić, Marin Kovacic, Hrvoje Kusic, Zlata Hrnjak Murgić, Dionysios D. Dionysiou, Panaghiotis Karamanis, Ana Loncaric Bozic

PII: S0048-9697(24)03491-0

DOI: https://doi.org/10.1016/j.scitotenv.2024.173344

Reference: STOTEN 173344

To appear in: *Science of the Total Environment*

Received date: 22 March 2024

Revised date: 7 May 2024

Accepted date: 16 May 2024

Please cite this article as: J.P. Zjačić, Z. Katančić, M. Kovacic, et al., Fragmentation of polypropylene into microplastics promoted by photo-aging; release of metals, toxicity and inhibition of biodegradability, *Science of the Total Environment* (2024), https://doi.org/10.1016/j.scitotenv.2024.173344

# Fragmentation of polypropylene into microplastics promoted by photo-aging; release of metals, toxicity and inhibition of biodegradability

Josipa Papac Zjacić[1], Zvonimir Katančić[1], Marin Kovacic[1], Hrvoje Kusic[1,2],* Zlata Hrnjak Murgić[1], Dionysios D. Dionysiou [3], Panaghiotis Karamanis[4], Ana Loncaric Bozic[1]

[1] Faculty of Chemical Engineering and Technology, University of Zagreb, Marulićev trg 19, 10000 Zagreb, Croatia

[2] University North, Trg dr. Žarka Dolinara 1, 48000 Koprivnica, Croatia

[3] Environmental Engineering and Science Program, Department of Chemical and Environmental Engineering, University of Cincinnati, Cincinnati, OH 45221-0012, USA

[4] Université de Pau et des Pays de l'Adour, E2S UPPA, CNRS, IPREM, Hélioparc Pau Pyrénées, 2 Rue de president Angot, 64053 Pau, France

To whom correspondence should be addressed:

*phone*: +385 1 4597 160 (*); *e-mail:* hkusic@fkit.unizg.hr (*)

**ABSTRACT**

The widespread presence of microplastics (MP) in water represents an environmental problem, not only because of the harmful effects of their size and potential to vector other pollutants, but also because of the release of additives, degradation products and residues contained in the polymer matrix. The latter includes metallic catalysts, which are often overlooked. This study focuses on the photo-aging of polypropylene (PP) and the resulting structural changes that promote its fragmentation microplastics (PP-MPs) and release of metals, as well as the resulting toxicity of leachates and their potential to inhibit biodegradation of organics in water. The pristine, photo-aged and waste PP are ground under the same regime to assess susceptibility to fragmentation. Obtained PP-MPs are submitted to leaching tests; the release of organics and metals is monitored by Total Organic Carbon (TOC) and Inductively Coupled Plasma Mass Spectrometry (ICP-MS) analysis, respectively. The leachates are assessed for their toxicity against *Vibrio fischeri*, *Daphnia magna* and *Pseudokirchneriella subcapitata* and their influence on the biodegradability of the glucose solution. Photo-aging induced changes in the crystallinity and morphology of the PP and manifested in the abundance of smaller MPs, as revealed by the particle size distribution. In the case of pristine PP, all particles were >100 μm in size, while aged PP yielded significant mass fraction of MPs <100 μm. The toxicity of leachates from aged PP-MPs is higher than that of pristine and exhibits a positive correlation with portion of metals released. The biodegradability of glucose is strongly inhibited by PP-MPs leachates containing a mixture of metals in trace concentrations.

**KEYWORDS**: microplastics; polypropylene; photo-aging; metals leaching; toxicity

**GRAPHICAL ABSTRACT:**

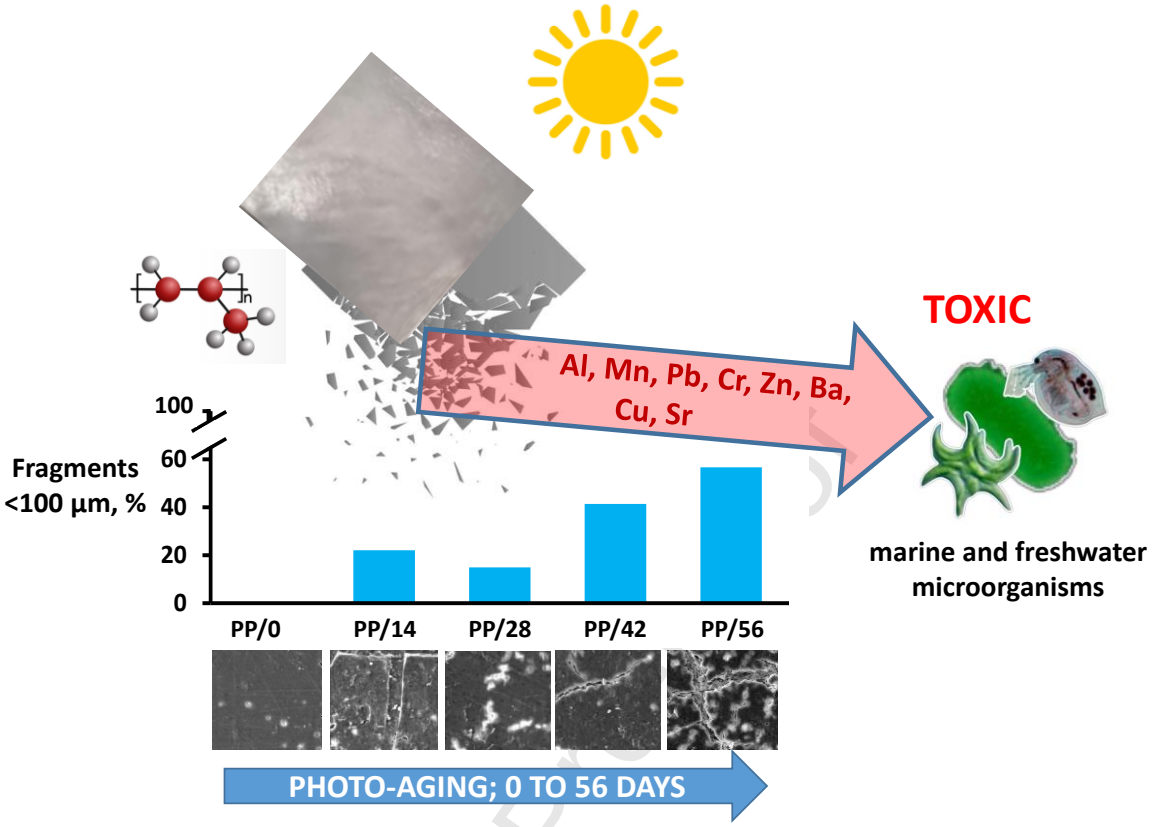

**HIGHLIGHTS:**

- Fragmentation of photo-aged PP results in a higher abundance of smaller MPs particles compared to pristine PP.
- Photo-aging increases the leaching rate of metals from PP-MPs.
- Leachates from aged PP-MPs exhibit higher toxicity in comparison to that of pristine PP-MPs
- Leachates from aged PP-MPs strongly inhibit biodegradability comparing to that of pristine PP-MPs

## 1. INTRODUCTION

Plastic materials have become an inevitable part of everyday life as they are used in various commercial materials and found application in many aspects of modern life such as packaging and food preservation, construction material for plumbing pipes, electronic devices, vehicles, etc. Besides polyethylene, polypropylene (PP) is the second-largest global plastic resin according to the production volume, with an estimated increase between 56-88 million tons for 2018-2026 period [1]. According to a recent policy scenario report provided by the Organization for Economic Co-operation and Development (OECD), global plastic use will be tripled by 2060, followed by a plastic waste increase from 353 to 1,014 million tons in 2060 [2]. An unwanted, but very common scenario is the inappropriate disposal of plastic waste in the environment where under various atmospheric conditions such as temperature, solar light, moisture [3], or even during the recycling process [4,5], plastic degrades and fragments into micro- and nano particles. Such phenomena are usually followed by the migration or leaching of additives and/or constituents from plastic waste [6]. Polymer additives are responsible for enhancing polymer properties and prolonging lifespan and include plasticizers, stabilizers, pigments, lubricants, antioxidants, flame retardants, and antimicrobial agents, while other constituent include monomers, intermediates, and catalysts emanate from polymerization as well as other contaminants introduced during the production and recycling process [7]. EU regulations for plastic materials are becoming more and more strict regarding the final products, as well as additives included to improve application properties, but may cause adverse effects to environment [8,9]. However, old persistent plastic litter containing hazardous compounds that are recently restricted will continue to pose an environmental problem for decades to come. Besides, such residues may contaminate new plastic materials through recycling process [10,11].

According to the literature, PP is one of the most frequently detected type of microplastics (MPs) in the environment [12]. Literature suggests that PP-MPs have the potential to induce adverse effects to organisms, such as digestive and metabolic issues, decrease of reproduction, and immune responses, while very rare are shreds of evidence regarding immobility and mortality [13]. Different aspects of MPs are responsible for the toxic effects they pose, including type, size and shape, adsorbed co-contaminants and leached constituents. Additives in PP are mostly pigments and stabilizers, while residues originated from Ziegler-Natta catalysts (used in synthesis) including metals and metalloids, such as Ca, Ti, Al, V, Cr, and Zr, and appearing in very low concentrations (e.g. 0.00005 mass% for Ti) may be also present [14]. Most of the current studies are focused on direct adverse effects that MPs pose, as well as those related to the release of MPs organic constituents and/or additives [3,6,12,15,16,19,20], while leaching of metals and metalloids is often overlooked and not duly considered. Adverse effects caused by heavy metals to aquatic organisms, plants and humans are well documented and reported [21-26], as well as their influence on biodegradability of organics co-contaminants in water [27,28].

This study focuses on the photo-aging of polypropylene (PP) and the resulting structural changes that prone fragmentation and promote release of metals from PP-MPs, as well as the resulting toxicity of aqueous leachates and their potential to inhibit the biodegradation of organics in water. Photo-aging of PP was performed in controlled laboratory conditions, studying changes in PP structure and morphology, and fragmentation into PP-MPs thereafter. MPs obtained from both pristine and photo-aged PP samples, along with MPs prepared from waste packaging PP collected from environment, were submitted to leaching tests in order to study release of metals and organics from the PP structure. The leachates were studied for their toxicity on marine bacteria *Vibrio fischeri*, freshwater crustacean *Daphnia magna*, and algae

*Pseudokirchneriella subcapitata*, and influence on biodegradability of readily biodegradable organic substrate D(+)-glucose in MPs leachates.

## 2. MATERIALS AND METHODS

### *2.1. Materials and Chemicals*

Polypropylene (PP) granules, Braskem, Europe GmbH (PP C765-15NA; density 0.900 g $cm^{-3}$, melt mass flow rate (MFR) 15 g / 10 min) were used to prepare pristine opaque PP films (denoted as PP/0 in further text), by pressing the granules using a hydraulic press (Dake, USA), temperature ($T$=190 °C) and pressure ($p$=34 bars), for 6 minutes, followed by 3 minutes of cooling at room temperature in a mold with the dimensions 19.0 × 8.0 × 0.2 cm. The obtained films were afterwards submitted to photo-aging. Pristine and aged films were characterized, ground into MPs, and used in further experiments. PP/0 was used as a benchmark to evaluate photo-induced changes of structural and morphological properties that influenced susceptibility of PP films to fragmentation when submitted to grinding under the same conditions. In addition, PP waste films from commercial food and cosmetic packaging (denoted as PP/A in further text) were collected from the environment (banks of the Sava River, Zagreb, Croatia), thoroughly washed to remove dirt and product residues, and dried. Visual inspection of the collected samples revealed surface cracks and color irregularities indicating the occurrence of environmental aging over an unknown period of time. Therefore, the PP/A samples were not subjected to accelerated photoaging and material characterization because reference, i.e. pristine material, was not available.

Nitric acid ($HNO_3$, p.a., Kemika d. d., Croatia) was used in preparation of samples for quantitative determination of metals in PP after combustion. Sulfuric acid ($H_2SO_4$, p.a., Kemika d. d., Croatia) was used to adjust the pH of the ultrapure water for the leaching tests. D(+)-glucose (p.a., GramMol, Croatia) was used as a readily biodegradable organic substrate to test

biodegradability. The experiments were performed with ultrapure water obtained with a Millipore Millipack (18.2 MΩ/cm, Direct Q-3, Merck Millipore, USA). Chemical kits used for the chemical (COD) and biochemical oxygen demand ($BOD_5$) test were purchased from Hach, Germany. In *Vibrio fischeri* (VF) toxicity tests, sodium hydroxide (NaOH, p.a., Kemika, Croatia) and sodium chloride (NaCl, p.a., Kemika, Croatia) were applied for pH and salinity adjustments, along with freeze-dried luminescent bacteria (BioFix Lumi Luminescent Bacteria, Macherey-Nagel GmbH, Germany). In *Daphnia magna* (DM) toxicity tests, sodium bicarbonate ($Na_2CO_3$, p.a., Lach-Ner, Croatia), calcium chloride dihydrate ($CaCl_2 \times 2H_2O$, p.a., Kemika, Croatia), magnesium sulfate heptahydrate ($MgSO_4 \times 7H_2O$, p.a., Kemika, Croatia), and potassium chloride (KCl, p.a., Lach-Ner) were used for the preparation of the freshwater medium. Powdered Spirulina was used for "pre-feeding" the test organisms prior to the toxicity test, while neonates are hatched from eppiphias and used as test organisms. In *Pseudokirchneriella subcapitata* (PS) toxicity tests, concentrated algal growth and culturing medium (MicrobioTox, Ghent, Belgium) was used for the preparation of samples at the desired dilution, along with the de-immobilized algal beads.

### *2.2. Photo-aging of PP films*

Photo-aging of PP/0 films was carried out in the SUNTEST CPS+ chamber (Heraeus Instruments, Germany), equipped with Xenon lamps (1500 W, Q-Lab, USA) and air cooling. The filter for cutting-off UV-C irradiation was applied, thus irradiation source simulated outdoor solar spectrum comprising UV-B, UV-A, and Vis irradiation (290-800 nm). The temperature in the chamber was controlled at 45±1 °C. The film samples were fixed in the chamber with a magnet and aged for 14, 28, 42 and 56 days; the photo-aged samples were denoted as PP/14, PP/28, PP/42, and PP/56, respectively. It should be noted that experiments were performed in triplicates in order to ensure reproducibility of results.

### *2.3. Characterization of structure and morphology of PP films*

Pristine and aged films (PP/0, PP/14, PP/28, PP/42, PP/56) were inspected for photo-induced structural and morphological changes employing Fourier transform infrared spectroscopy (FTIR), diffuse reflectance (DRS) spectroscopy and differential scanning calorimetry (DSC), and scanning electron microscopy (SEM), respectively. The FTIR spectra were recorded by a Spectrum One (Perkin Elmer, USA) using attenuated total reflection (ATR) with ZnSe crystal in the range from 4000 $cm^{-1}$ to 650 $cm^{-1}$. The carbon-oxygen bond, C.I.(C-O), and carbonyl group bond, C.I.(C=O), indexes were calculated employing equations (1) and (2), respectively [29,30]. Hence, C.I.(C-O) was determined as ratio of carbon-oxygen peak between 1140 and 1240 $cm^{-1}$ and a reference peak of methylene ($CH_2$) between 1500 and 1425 $cm^{-1}$. C.I.(C=O) was determined as a ratio of carbonyl group peak between 1830 and 1680 $cm^{-1}$ and a reference peak of methylene ($CH_2$) between 1500 and 1425 $cm^{-1}$.

$$\mathrm{C.I.\,(C-O)} = \frac{\text{Area under band } \mathrm{A}_{1240-1140\ \mathrm{cm}^{-1}}}{\text{Area under band } \mathrm{A}_{1500-1425\ \mathrm{cm}^{-1}}} \quad (1)$$

$$\mathrm{C.I.\,(C=O)} = \frac{\text{Area under band } \mathrm{A}_{1830-1680\ \mathrm{cm}^{-1}}}{\text{Area under band } \mathrm{A}_{1500-1425\ \mathrm{cm}^{-1}}} \quad (2)$$

The area under the band was calculated employing the software options from the peak analysis tool. DRS spectra were recorded using UV-VIS spectrometer 2600i (Shimadzu, Japan) with an ISR-2600Plus accessory in the wavelength range of 200-800 nm and a resolution of 1 nm, employing barite ($BaSO_4$) as the white standard. DSC analysis was performed using a differential scanning calorimeter (Mettler Toledo DSC 823eT, USA) in three cycles: (i) cooling/heating from 25 °C to 200 °C, (ii) cooling from 200 °C to -70 °C, and (iii) reheating from 25 °C to 200 °C, at a heating/cooling rate of 10 °C/min. The degree of crystallinity ($X_c$) was determined according to equation (3), as the ratio of the enthalpy of melting of the studied samples ($\Delta H_m$) and the sample with a crystallinity of 100% ($\Delta H_m^0$), which was taken as the literature value of 207 J $g^{-1}$ for isotactic polypropylene (i-PP) [31]:

$$X_C = \frac{\Delta H_m}{\Delta H_m^0} \quad (3)$$

SEM images were recorded by Tescan Vega III (Tescan, Czech Republic) at 10 kV. Before the inspection of the sample, the surface was coated with EMS 550X sputter coater under a high vacuum by sputtering gold/palladium (60:40) to achieve conductivity.

The PP/A samples were subjected to FTIR analysis to confirm the assumption that the collected packaging waste samples were polypropylene films. However, they were not further characterized by DRS, DSC and SEM analyses for photo-induced changes as they were not aged under controlled conditions but collected from the environment.

### *2.4. Preparation of microplastics and particle size distribution*

Pristine and aged films (PP/0 and PP/14, PP/28, PP/42, PP/56, respectively) were cut into the dimensions 0.5 cm × 0.5 cm and thereafter ground in a single-drum cryogenic mill (Retsch, Germany) to obtain micro-sized particles. Grinding was performed in three cycles, each cycle consisted of three steps: precooling ($f$=5 $s^{-1}$; $t$=30 s), milling ($f$=15 $s^{-1}$; $t$=30 s), and intermediate cooling ($f$=5 $s^{-1}$; $t$=30 s). After the third grinding cycle, the particles were separated according to their size employing a sieve shaker with five sieves of different mesh sizes (Sieve Shaker AS 200 control, Retsch, Germany). The following fractions were obtained: >500 µm, 400-500 µm, 300-400 µm, 200-300 µm, 100-200 µm, and <100 µm and their mass fractions (mass %) for each sample were determined gravimetrically. In order to study the influence of photo-aging on susceptibility of PP to fragmentation, a particle size distribution was determined for PP-MPs/0, PP-MPs/14, PP-MPs/28, PP-MPs/42, and PP-MPs/56 samples. PP-MPs/A were prepared from a mixture of waste packaging films, applying the same grinding procedure. Particle size distribution was not reported because the waste films were not photo-aged under controlled conditions but were collected from the environment. However, it should be noted that PP-MPs/A particles obtained by grinding had a size of < 500 µm.

### *2.5. Leaching test*

To elucidate the influence of aging on release of organics and metals from PP-MPs, PP-MPs/56, aged for the longest period, was submitted to leaching test, whereas PP-MPs/0 was used as benchmark. In addition, MPs prepared from waste PP aged for unknown period in environment (PP-MPs/A) (Table 1), was submitted to leaching tests, however without a benchmark as its pristine material was not available.

Table 1. PP materials used to prepare MPs samples employed in leaching experiments

| PP/0 | PP/56 | PP/A |
|---|---|---|
|  | 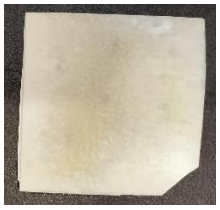 |  |

The experiments were performed according to modified procedures described elsewhere [31-34]. Hence, ultrapure water ($V$=20 mL) adjusted with 0.1 M $H_2SO_4$ at pH 6 was used as the leaching medium, containing mentioned MPs in concentration of 100 g $L^{-1}$. The suspension was incubated at 40 °C for 10 days in an orbital shaker OLS Aqua Pro (Grant, UK), and then filtered using PTFE filter (0.45 μm, Macherey Nagel, Germany). The obtained filtrate was used to determine the leached organics and metals.

The filtrates from leaching tests of PP-MPs/0, PP-MPs/56 and PP-MPs/A were submitted to TOC analysis using Total Organic Carbon analyzer, TOC-$V_{CPN}$, Shimadzu, Japan, to determine the potential differences in the release of organics from pristine, aged and waste PP (PP-MPs/0, PP-MPs/56, and PP-MPs/A, respectively).

To determine the types and concentrations of metals present in studied PP-MPs materials prior leaching test, the samples (10 g) were fully combusted in ceramic crucible employing muffle furnace LHT 08/18/P310 (Nabertherm, Germany) at 550 °C for 3 hours. The residue obtained was suspended in 1 mL of $HNO_3$ (65 v/v%) and then 100 mL of ultrapure water was added.

The obtained suspension was then filtered using PTFE filter and concentrations of present metals were determined.

The qualitative and quantitative analysis of metals in both studied PP-MPs materials and in filtrates after leaching tests was determined using Inductively Coupled Plasma Mass Spectrometry (ICP-MS), ICP-MS 7800 (Agilent, USA), equipped with a standard one-piece extended torch with a quartz injector tube, a concentric spray chamber, and a concentric nebulizer. The operating parameters were radio frequency power of 1550 W and coolant, auxiliary, nebulizer, and collision cell gas with flow rates at 14 L Ar $min^{-1}$, 0.8 L Ar $min^{-1}$, 1.05 L Ar $min^{-1}$, and 5 ml He $min^{-1}$, respectively. The reagent (2 w/v % $HNO_3$) and 1000 µg $mL^{-1}$ standards (Al, As, Ba, Ca, Cu, Cr, Fe, K, Mg, Mn, Na, Ni, Pb, Sr, V, Zn) were purchased from Trace Analysis Grade (Merck, Germany).

The aliquot of aqueous samples was 20 ml and measurements were carried out in triplicates, reporting the average value (reproducibility was 97.1%).

***2.7. Aquatic toxicity tests***

Toxicity tests were performed on aqueous samples obtained after leaching tests and were conducted according to the standard procedures disclosed in ISO 11348-3:2007 [35], ISO 6341:2012 [36], and ISO 8692:2012 [37] for following toxicity test organisms: (i) standard luminescent bacteria test to determine the inhibitory effect of water samples on the light emission of *VF*, (ii) standard freshwater test to determine the inhibition of the mobility of *DM Straus* (Cladocera, Crustacea), and (iii) freshwater algal growth inhibition test with unicellular green algae *PS* (*Selenastrum capricornutum*), respectively.

For this purpose, freeze-dried bacteria *VF*, and DaphToxkit and Algaltoxkit F, were purchased from Macherey Nagel, Germany, and Microbiotest, Belgium, respectively. The samples for toxicity tests were collected after leaching tests performed in slightly acidic medium (pH 6); thus, the pH value was adjusted to 7 prior toxicity tests. In the case of the toxicity test to *VF*,

2% NaCl was added to the samples (to simulate marine environment), while in the case of *DM* and *PS* tests, specific media were prepared according to protocols [36,37]. Test batches were incubated for 15 minutes for *VF*, 48 for *DM*, and 72 hours for *PS*.

The luminometer BioFix Lumi-10 Toxicity Analyzer, Macherey-Nagel, Germany) was used to measure the photoluminescence of *VF*, the light table was used to follow the immobilization of *DM*, and a spectrophotometer with a holder for the cells of 10 cm path length (Jenway 6200, UK) was used for the algae test.

The measurements were carried out in triplicates, reporting the average value (reproducibility was 97.9%).

### *2.8. Biodegradability*

The influence of leached metals and organic constituents of studied PP-MPs samples was investigated against changes in biodegradability of the readily biodegradable organic substrate, D(+)-glucose. Namely, glucose is a part of standard $BOD_5$ substrate, along with glutamic acid [38]. Hence, glucose (10 mg $L^{-1}$) was added to the filtrate collected upon leaching tests. Biodegradability was estimated based on $BOD_5$/COD ratio. Chemical (COD) and biochemical oxygen demand ($BOD_5$) were determined by colorimetric methods using HACH DR2800 spectrophotometer (Hach-Lange, USA) and Lange reagent kits LCK414 (for COD; based on dichromate oxidation, conditioned for 2 h on 170 °C) and LCK554 (for $BOD_5$; based on the inhibition of nitrification by allylthiourea, conditioned for 5 days at 20 °C). It should be noted that COD values determined for mixtures of glucose and leachates were corrected for COD determined in leachates only, since metals can contribute to the overall COD values. The measurements were carried out in triplicates, reporting the average value (reproducibility was 97.3%).

## 3. RESULTS AND DISCUSSION

### *3.1. Characterization of structural and morphological properties of PP films*

Fig. 1. shows FTIR spectra of PP films; PP/0 (pristine) and PP/14, PP/28, PP/42, and PP/56 (photo-aged for 14, 28, 42 and 56 days, respectively). Taking into account that UV irradiation is considered a main contributing factor in the degradation of plastics [39,40], the UV dose received by the samples can be used to extrapolate accelerated laboratory to environmental conditions. Hence, we applied the methodology from our previous study to estimate the local average outdoor UV dose using UV irradiance data obtained from the meteorological service [41]. Hence, the accelerated ageing of PP films applied in this study during 14, 28, 42 and 56 days roughly corresponds to 476, 952, 1428 and 1904 days of environmental ageing in the southern part of Central European area. Characteristic peaks for PP polymer can be observed, exhibiting its original chemical composition, as well as the chemical transformation occurring after photodegradation (for aged samples only). The peaks at 2953, 2916, and 2836 $cm^{-1}$ correspond to the asymmetric C−H stretching of $-CH_2$ and $-CH_3$ groups, while the peaks at 1462 and 1377 $cm^{-1}$ correspond to the symmetric bending of $-CH_3$ groups. Furthermore, the peaks at 998, 974, 842, and 1172 $cm^{-1}$ define the isotactic structure of PP molecules, corresponding to C−C and C-H bonds in the basic chain (Table S1, Supplementary material) [42,43]. These characteristic peaks for PP can be also observed in the case of PP/A samples (Fig. S1, Supplementary Material).

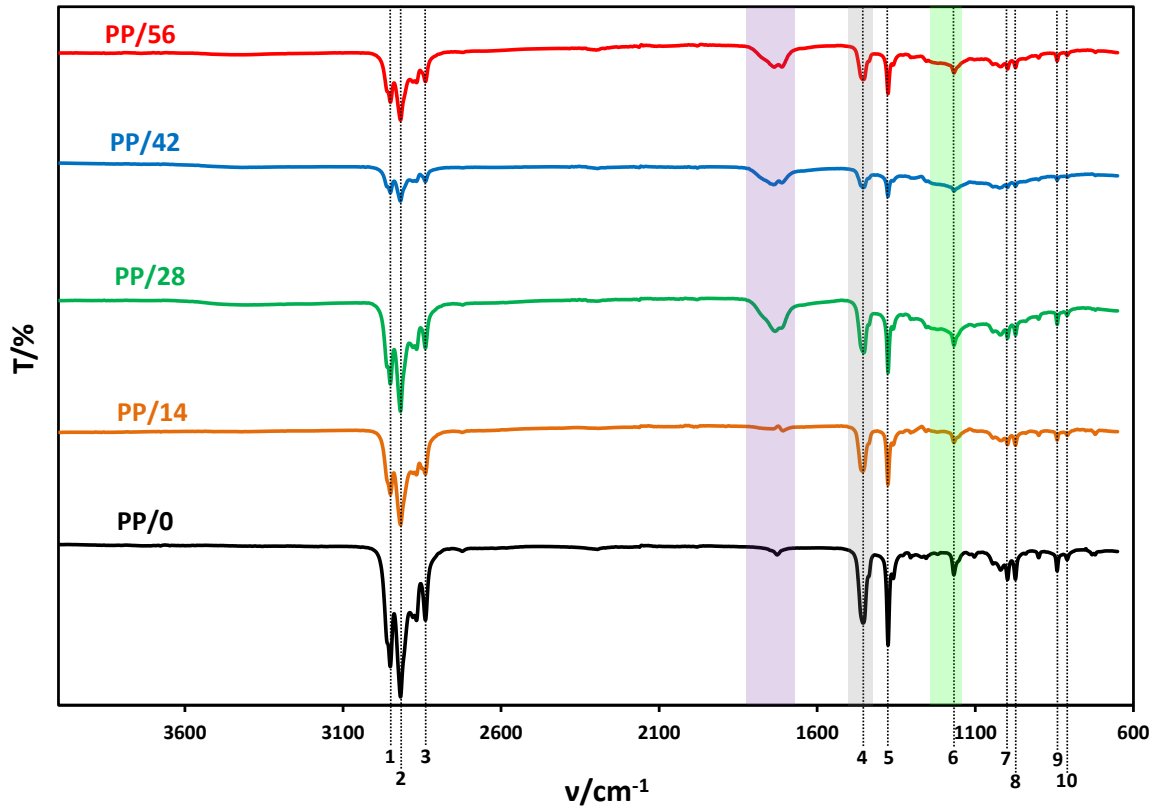


**Figure 1**. FTIR spectra of PP/0, PP/14, PP/28, PP/42, and PP/56; (i) vertical dash lines correspond to numbers listed in Table S1 (first column), and (ii) marked area with green, magenta and gray correspond to areas used to calculate CI (C-O), CI(C=O) and referent one

In the samples photoaged for 28 days or more (PP/28, PP42, PP56, Fig. 1), the appearance of new peaks at 1744 and 1725 $cm^{-1}$ can be observed (region marked with transparent magenta color in Fig. 1.). Those correspond to newly formed carbonyl groups (C=O). Oxidation of PP occurs by a chain reaction of free radicals upon excitation by UV radiation (UV-B and UV-A are part of the simulated solar light induced in our case), leading to the homolytic splitting of the covalent C-H and/or C-C bond in PP chain. The reaction of the free radical (R•) with oxygen generates peroxy radicals (ROO•) and then hydroperoxides (•OOH), which are further decomposed forming an alkoxy radical (RO•). It is considered that the oxidative scission of the chain occurs by the decomposition of this alkoxy radical into two molecules; one ends the chain forming a keto group, while another undergoes in new reaction cycle, as described by reaction

mechanism of Norrish I and Norrish II (Fig. 2) [44,45]. Surrounding "environment" of the carbonyl group in the molecule causes a shift of peak maximum. If C=O is located at the end of the chain, then it corresponds to the vibrations at 1725 $cm^{-1}$.

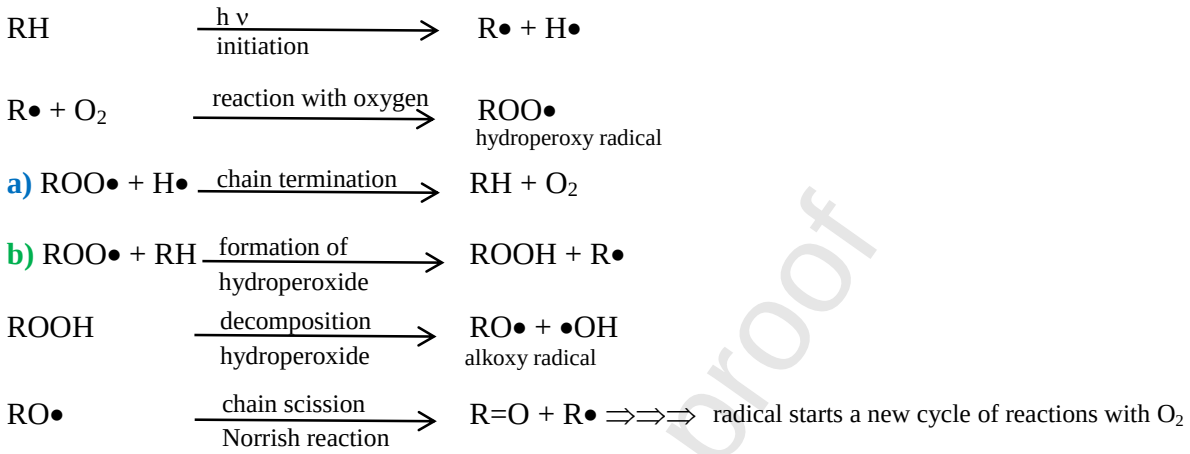


**Figure 2**. General schemes of mechanism of photooxidative degradation of PP.

In the case of its placement in the middle of the molecule, the peak shifts to 1744 $cm^{-1}$ (Fig. 1.). Carbon-oxygen bonds (C–O, O–C=O, C–O–O–), with absorbance intensity ranging from 1140 to 1240 $cm^{-1}$ (region marked with transparent green highlighting in Fig. 1.) were used along with carbonyl group (C=O) as a measure of photodegradation of PP films during photo-aging. To quantify the degree of photodegradation, carbon-oxygen and carbonyl group indexes (C.I.(C-O) and C.I.(C=O), respectively) were calculated (equations (1) and (2)), and the values are summarized in Table 2 [29,46].

Table 2. Indexes of the carbonyl group and the carbon-oxygen bonds

| Samples | Carbonyl group, C = O | Carbon-oxygen, C – O |
|---|---|---|
| **PP/0** | 0.1094 | 0.3730 |
| **PP/14** | 0.5157 | 0.9765 |
| **PP/28** | 1.4155 | 1.6039 |
| **PP/42** | 1.8244 | 1.8045 |
| **PP//56** | 1.6295 | 1.6118 |

The results indicate that intense photo-aging of PP films occurred; the values of C.I.(C=O) increased significantly compared to the initial one. For example, after 56 days of photo-aging a 15-fold increase of C.I.(C=O) was recorded. Simultaneously, C.I.(C-O) value was 4-folded compared to that of pristine sample (Table 2). According to the literature [47], and the mechanism of oxidative degradation (Fig. 2.), it is obvious that simulated solar light initiated polymer degradation. Namely, UV fraction within simulated solar light (UV-B and UV-A) possess the energy of 315–400 kJ $mol^{-1}$, which is sufficient to cleave C–C and C–H bonds in polymer molecules. Moreover, the degradation involves the scission of polymer macromolecules resulting in the formation of a large number of low molecular weight polymers (oligomers), causing also the structural transformation of molecules leading to formation of carbonyl and carbon-oxygen groups (Fig. 1). However, as reported by Rouillon et al. [48], the C.I.(C=O) is not absolute quantitative probe to monitor polypropylene photodegradation, but can be considered as indicator of structural changes due to PP degradation and need to be supplemented by crystallinity evaluation and qualitative and/or quantitative analysis of leached organics, which we employed further in the study. The above discussed structural changes in polymer molecules would lead to significant variations of polymer properties, such as the alteration of strength and an increase in brittleness, which, in turn, allow an easier and faster fragmentation of polymers, a starting point for MPs generation in the environment.

Fig. 3 shows UV-Vis DRS absorption spectra (200 to 800 nm) of pristine and photo-aged PP films, recorded to elucidate transformation of molecular changes caused by photodegradation, thus impacting properties and behavior of plastics. The peaks on DRS spectra between 200 - 220 nm correspond to $n - \sigma^*$ or $\pi - \pi^*$ transition in organic functional groups, while the absorption peak at 220 nm corresponds to the diene group. Those appeared in the spectra of all PP films studied, and are formed during synthesis and processing, and may serve as a starting sites for the initiation of chemical degradation during the exposure to solar light

[49,50]. The main difference in photo-aged samples occurred in the range between 260 and 340 nm (Fig. 3). It should be noted that the absorbance in the range between 260 and 290 nm is usually due to the $n - \pi*$ electron transition in oxygen-containing species that are present in the most conjugated molecules [51]. Accordingly, it can be concluded that different types of C–O groups are formed on the surface of PP films during photo-aging; e.g. C=C–C=O at 220 nm, C=O at 280 nm, C=C–C=O at 290 nm and simultaneous oxidative functionalities such as –C–O–, –COO–, –COH–, O–C=O–, –COOH absorbing in the range between 280 and 290 nm. The absorption at 340 nm and above 400 nm, which increases with the increase in period of photo-aging, indicates the formation of conjugated chromophores sensitive to color changes in the visible spectral range. Such an effect is particularly visible in PP/42 sample (Fig. 3). In the case PP/56 sample, which was exposed to photo-aging over the longest period (56 days), three distinct peaks with a maximum ($\lambda_{max}$) at 232, 280 and 320 nm can be clearly observed (Fig. 3). The peaks at $\lambda_{max}$=232 nm and $\lambda_{max}$=320 nm correspond to unsaturated ketones [52]. The absorption maximum with shorter wavelength corresponds to the transition of $\pi$-electron, while the maximum with longer wavelength and weaker intensity corresponds to the transition of non-bonding electrons at the carbonyl oxygen atom [53]. According to the mechanism of Norrish I and II reactions (Fig. 2), different C–O groups are formed in PP film samples, indicating scission of the polymer molecule due to photodegradation of the polymer chain during photo-aging [34].

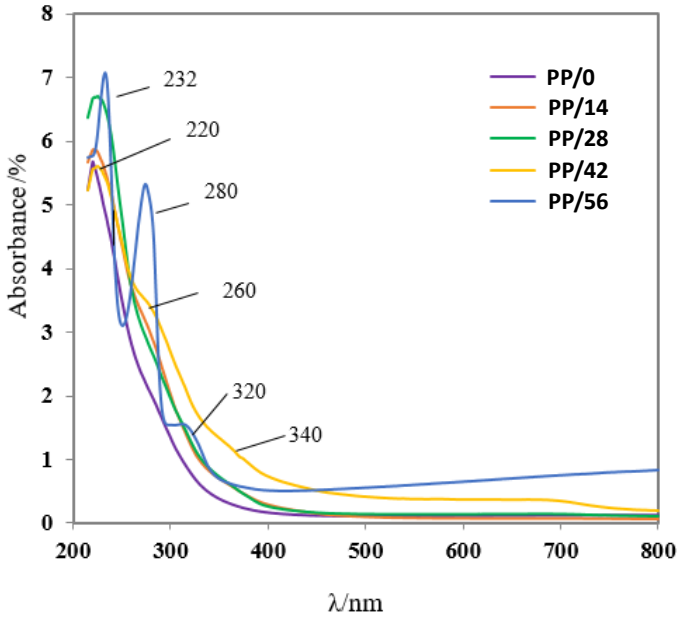


**Figure 3**. DRS spectra of PP film samples; pristine and photo-aged for 14, 28, 42 and 56 days.

DSC was employed to study the effects of structural changes caused by photodegradation on the thermal properties and crystallinity behavior of PP films. DSC thermograms are showed in Fig. 4(A) and (B), while the degree of crystallinity ($X_c$) as a function of exposure time, which was calculated from the enthalpy of fusion ($\Delta H_m$) using equation (3), is showed in Fig. 4(C). The photodegradation of PP films resulted in materials with a shift of the melting temperature ($T_m$) to lower values compared to that of the pristine sample. As can be observed, $T_m$ values were lower as photo-aging period was longer (Fig. 4(B)). This could be attributed to the reorganization of macromolecular chains into structures possessing lower melting point, thus shifting the main endothermic peak (168 °C), corresponding to the long chains in pristine PP, to lower values [48]. As exposure to photo-aging was prolonged, the appearance of an additional peak in the range of 145-135 °C was noticed (Fig. 4(B)). It should be noted that in PP/56 sample such newly appeared peak is even more emphasized than the

shifted main endothermic peak. This phenomenon is consistent with the mechanisms of chain scission, suggesting that prolonged photo-aging leads to the degradation of the polymer chains.

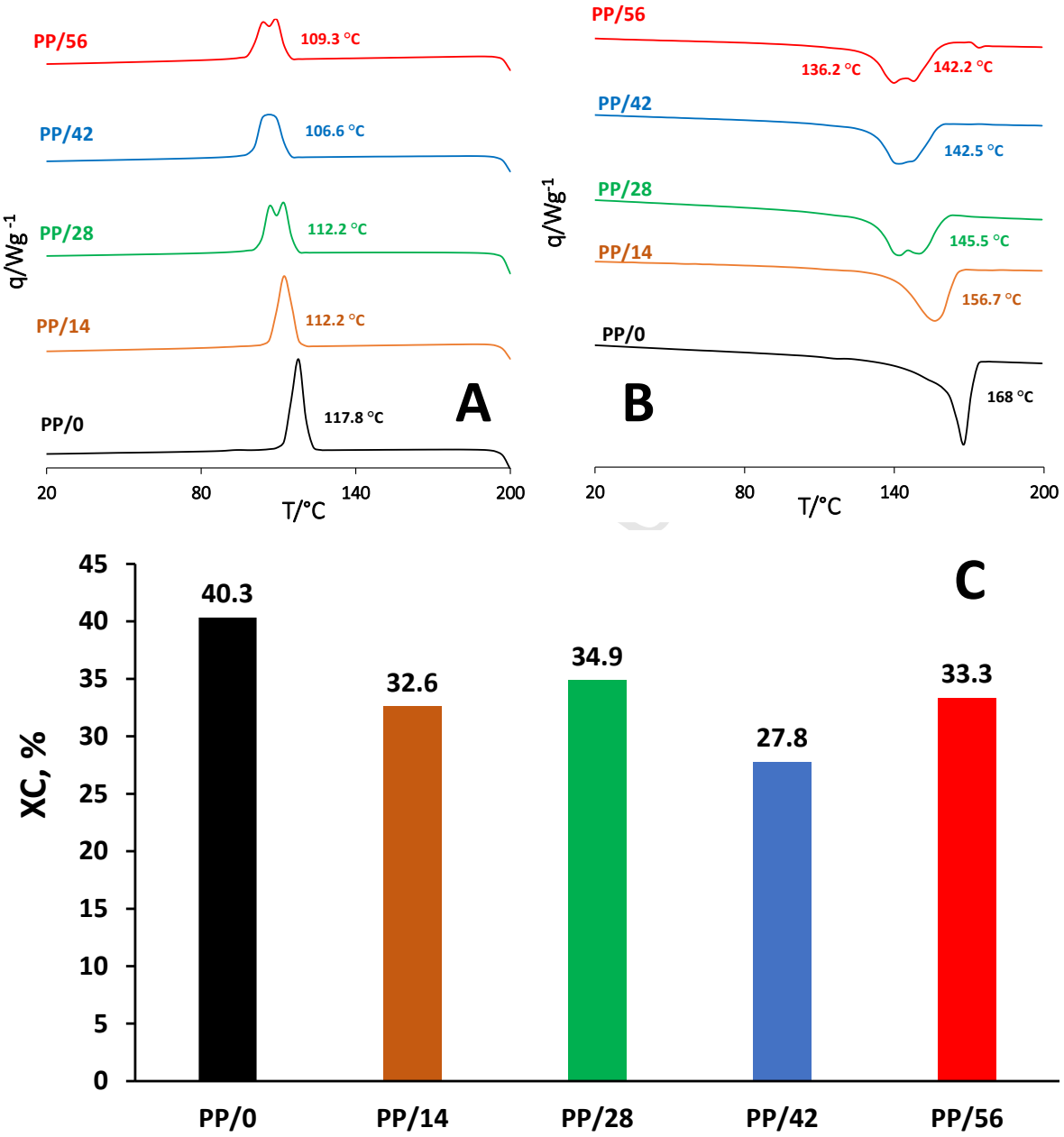


**Figure 4**. DSC thermograms of pristine and photo-aged PP film samples showing melting temperature ($T_c$) (A), and crystallization temperature ($T_m$) (B), and the crystallinity index ($X_c$) of pristine and photo-aged PP films (C).

Accordingly, in PP/56 sample the main peak, $T_m$, broadened the temperature range of melting, starting at 125 °C and ending at 142°C, suggesting an increase in the mobility of the chains.

This is consistent with a mechanism involving chain scission and the formation of oligomers (polymers with lower molecular mass) formed by the Norrish I mechanism (Fig. 5) [54,55].

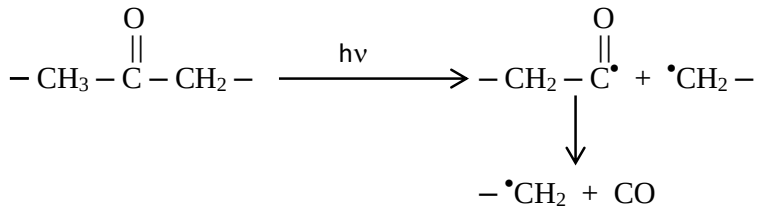


**Figure 5.** Typical Norrish I mechanism.

The same behavior is observed during cooling, which indicates the transition of the material from melt to solid, i.e. crystallization occurs. Even after severe chemical degradation induced by photo-aging, the ability of PP to crystallize remained, but with a lower degree of crystallinity and a lower crystallization temperature ($T_c$) (Fig. 4(B)). The photodegraded PP shows similar crystallization behavior as PP with impurities [56]. The presence of the low molecular weight polymer chains, formed during photodegradation, acts as a defect causing partial crystallization in separate phases. Hence, the crystallization of photodegraded PP occurred in two phases, which could be due to the segregation of molecules of similar size (e.g., small chains separated from large ones) forming a separate distinct crystal phase (separate domains), as shown by the double peaks (Fig. 4(B)) [57]. In addition, the degree of crystallinity ($X_c$) is lower for 20-30% in the cases of photo-aged PP films comparing to pristine one (Fig. 4(C)). According to the literature [58-60], photodegradation of PP can be lead to the chain scission and/or branching due to the formation of free radicals, possessing higher mobility. Chain scission would contribute to the increase of crystallinity, while branching leads to the opposite effect. According to the results presented in Fig.4(C), it seem that branching is more dominant in our case.

SEM analysis of pristine and photo-aged PP films surface was performed, and results are presented in Fig. 6.

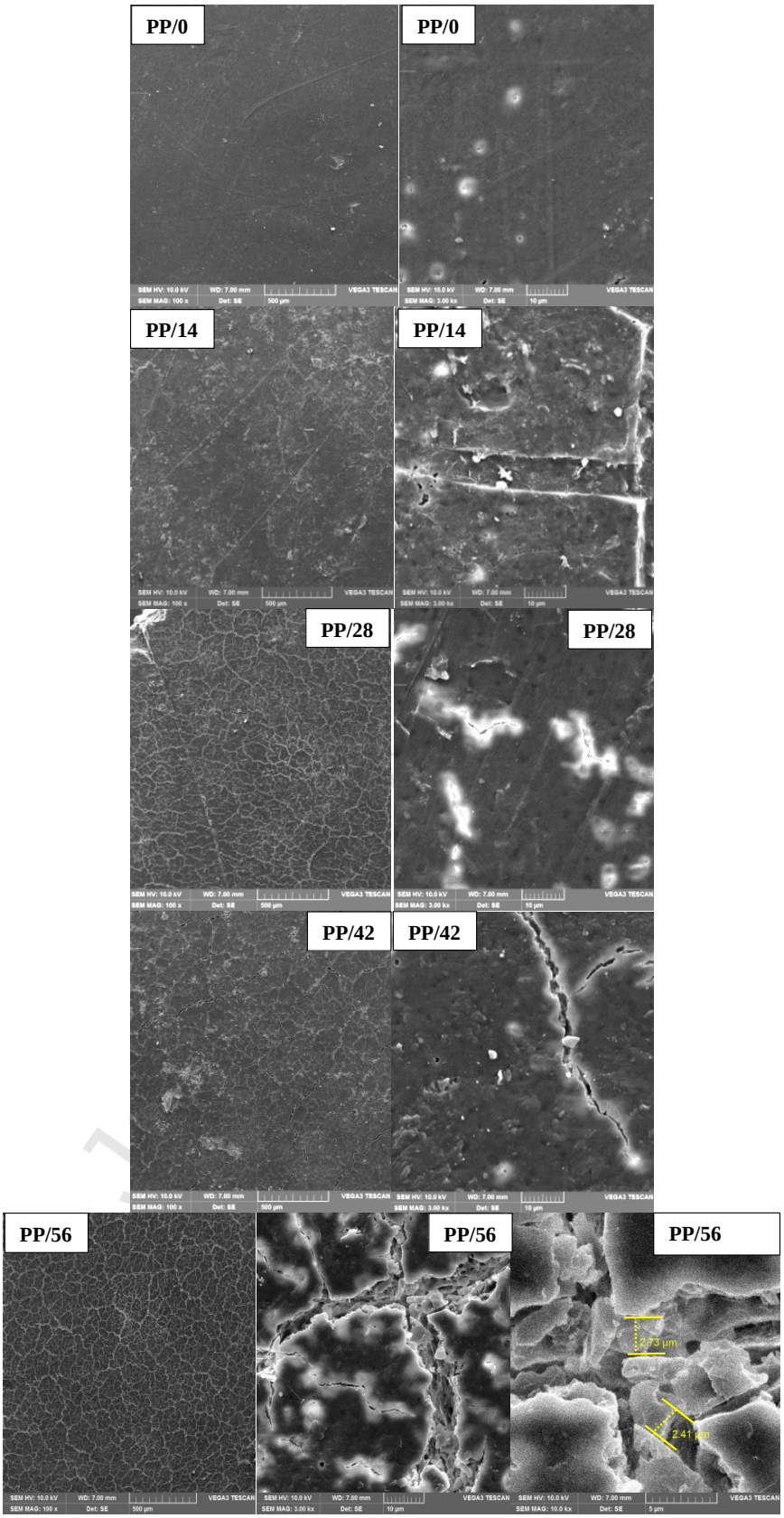


**Figure 6**. SEM micrographs of pristine (PP/0) and photo-aged PP films (PP/14, PP/28, PP/42 and PP/56)

The formation of surface cracks and scars can be observed on the surface, even at low magnifications (100x, left side of Fig. 6). At higher magnifications (3000x, right side of Fig 6.), cracks and scars are even more visible, e.g., the size of the cracks in PP/56 is about 2.41 - 2.73 μm (Fig. 6, bottom row, most right position). It is evident that photodegradation has induced cracks on the surface and increased the embrittlement of the polymer, as the cracks act as micro-scars for the fracture of the material under mechanical stress. The tendency of surface contraction combined with the decrease in average molecular mass ultimately leads to the formation of surface cracks, even without applied stress [61].

### *3.2. Fragmentation of PP films into MPs and leaching tests*

After photo-aging, PP films were grinded in a cryomill to analyze their fragmentation into smaller particles and to correlate with increased embrittlement caused by photodegradation. The particles were sieved with a series of sieves whose size range was between 100 and 500 μm. The particle size distribution *vs* photo-aging period is presented in Fig. 7., as well as their mass fractions (mass %). Comparison of the pristine and photo-aged PP films shows that the particle size distribution is significantly different (Fig. 7). Thus, the pristine sample (PP/0) does not possess particles <200 μm, while the largest fraction are particles in size of 300 to 400 μm (37 mass %). Besides, PP/0 sample comprises even 20 mass% of particles with a size of >500 μm. On the other hand, the samples photo-aged for 42 and 56 days (PP/42 and PP/56) have large fractions of particles of very small size, <100 μm (41 and 57 mass%, respectively), as well as very low fraction of particles with a size >500 μm (6 and 3 mass%, respectively). This significant change in particle size distribution suggest increased brittleness of aged samples, in spite of lower crystallinity (Fig. 4(C)). The same effect was observed by Uheida et al. [55], where photodegradation of PP lead to decrease of melting point with the prolonged treatment time, as well as generation of PP-MPs of smaller sizes.

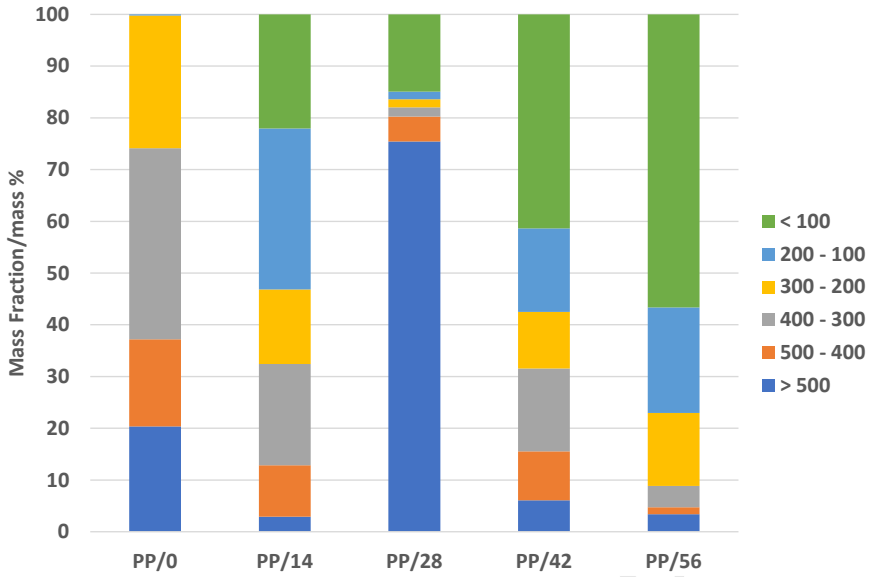


**Figure 7**. Particle size distribution (µm) and mass fractions (mass %) of grinded pristine and photo-aged PP films.

The leachates from PP-MPs/0, PP-MPs/56 and PP-MPs/A, were analyzed for organic content and metals. TOC analysis revealed that all three PP-MPs samples released low amounts of organics under test conditions. In all cases TOC values were <1 mg C $L^{-1}$. Pristine PP used in this study was a high performance impact copolymer developed for injection molding applications and contains nucleating agents and antistatic additives. Besides common inorganics such as talc and barium sulphate or montmorillonite nanoclays, nucleating agents may also include organic phosphates, carboxylates and sorbitoles, while common antistatic agents include long-chain aliphatic amines and amides, quaternary ammonium salts, esters of phosphoric acid, polyethylene glycol esters, or polyols. Accordingly, in the case of PP-MPs/0, it is expected that organic content in leachates originate from organic additives. However, due to low amounts of additives contained in PP/0 samples and relatively mild conditions of the leaching tests, the observed TOC was less than 1 mg C $L^{-1}$. On the other hand, it is known that photo-aging of polymer material may be associated with formation of low molecular weight organic products that may be released into the water [19,20,55]. However, obtained results

indicated that accelerated photo-aging applied in this study did not yield the degradation extent that would allow for observable differences in TOC values of PP-MPs/0 and PP-MPs/56 leachates, but PP-MPs/A as well. It is known that the most of potential by-products of photodegradation of PP are volatile [55]. Thus, taking into account the fact that our leaching test were performed in open system, low detected TOC values are not surprising.

In order to determine the content of metals present in starting materials prior to leaching tests, PP-MPs/0 (as a pristine material of photo-aged PP-MPs/56 sample) and PP-MPs/A samples were submitted to combustion to identify the type and quantity of metals present (Table 3). Since PP-MPs/0 and PP-MPs/56 samples were prepared from pristine PP polymer, metals originated from catalysts employed for PP synthesis were expected to be found. Several Ziegler-Natta (ZN) catalysts can be used to produce PP through vast array of processes [62,63]. From the results presented in Table 3, it can be concluded that ZN catalyst in studied PP polymer consists of $TiCl_3$, $TiCl_4$, and $MgCl_2$ activated by the addition of an organoaluminum co-catalyst, typically triethylaluminum ($Al(C_2H_5)_3$, i.e. TEAL) or $VOCl_3$-$Al(C_2H_5)_3$. Titanium-magnesium ZN catalysts are the basis of modern PP production processes, while iron oxide (FeO) is a compound that can be used as a new support. However, the latter can be also found as a residue of reactor maintenance and/or equipment cleaning [63-65]. As can be seen from Table 3, PP-MPs/0 exhibited Ti, Al and Mg metals in higher concentration and co-catalysts V and Fe in lower concentration, while the presence of Ca can be considered as a residue of the neutralizing compound added at the end of PP synthesis. Other metals detected in PP-MPs/0 sample can be considered as impurities, i.e. non-intentionally added substances (NIAS), present in very low concentration. On the other hand, in PP-MPs/A sample, which was prepared from waste packaging PP collected from the environment, concentrations of most of detected metals are double or even higher compared to those in PP-MPs/0 (Table 3). Exceptions are Mg, Fe and V, present in lower concentrations comparing to pristine PP sample (PP-MPs/0). It should be noted

that PP-MPs/A contains particularly high content of Al, Ba, Sr, and Ca. Plausible explanation for high content of Ba, and partially Ti, is that those metals are used in white pigments. The high content of Sr, which is a part of reddish pigments, can be explained in similar manner. Namely, different than opaque PP/0, PP/A were colored (Table 1). The increased Ca concentration can be explained by the presence of filler ($CaCO_3$), while Al presence is likely due to contamination. Additionally, the higher concentrations of metals in PP-MPs/A sample may be attributed to the additional treatments, specific for final products.

The results of significant leaching of metals from PP-MPs/0, PP-MPs/56, and PP-MPs/A samples after exposure to simulated acidic aqueous environment for 10-days are presented in Table 3, in both absolute values (μg $L^{-1}$) and relative (%) to overall content present in solid samples. The results obtained for pristine sample (PP-MPs/0) exhibited presence of monitored metals in rather low concentrations in the leachate studied, up to 5% (Ni) of overall present in PP-MPs/0 solid sample. It should be noted that some of the metals present in PP-MPs/0 sample were not detected in leachate (Al, Fe, Ca, Pb, Cr, Mn and Sr), indicating their stability in polymer material against slightly acidic conditions applied in the performed leaching tests. On the other hand, in the leachate of PP-MPs/56 sample, i.e. photo-aged sample, all monitored metals were detected, and moreover, in significantly higher values comparing to its pristine analogue (PP-MPs/0). Hence, in some cases (Pb, Ni, Zn, and Cu) values detected in leachate are close to 100 %, meaning that almost all present metals in PP material leached. Such results indicate the migration of metals from both the surface and the bulk of polymer, presumably due to severely damaged PP structure during photo-aging, as proven through the above-presented and discussed characterization results. Hence, the obtained results suggest that plastics remained in the environment for longer period undergo aging and consequently, metals would be released. In the case of PP-MPs/A leachate, leached fractions of metals were generally higher than those recorded for pristine PP sample (PP-MPs/0) (Table 3). However, again Al, Fe, Cr

and As were not detected in leachate, indicating their stable incorporation into polymer during the polymerization process.

Table 3. Concentrations of metals in solid samples (PP-MPs/0 and PP-MPs/A) and those leached from PP-MPs/0, PP-MPs/56, and PP-MPs/A detected and quantified by ICP-MS analysis.

| metal | Concentration of metals in solid sample, mg $kg^{-1}$ | | Concentration of metals in water (after leaching test), µg $L^{-1}$ | | | leached portion, % | | |
|---|---|---|---|---|---|---|---|---|
| | PP-MPs/0 | PP-MPs/A | PP-MPs/0 | PP-MPs/56 | PP-MPs/A | PP-MPs/0 | PP-MPs/56 | PP-MPs/A |
| Ti | 32.46 | 58.71 | 40.81 | 68.2 | 117.35 | 1.26 | 2.10 | 2.00 |
| Al | 60.72 | 112.39 | - | 698.67 | - | - | 11.51 | - |
| Mg | 841.5 | 209.4 | 3.107 | 971.97 | 32.62 | 0.004 | 1.16 | 0.16 |
| Fe | 23.38 | 13.78 | - | 103.96 | - | - | 4.45 | - |
| V | 0.080 | 0.053 | 0.001 | 1.168 | 0.414 | 0.01 | 14.60 | 7.81 |
| Ca | 56.34 | 810.50 | - | 2342.01 | 358.31 | - | 41.57 | 0.44 |
| Pb | 0.018 | 0.088 | - | 1.796 | 0.031 | - | 99.78 | 0.35 |
| Cr | 0.440 | 0.806 | - | 0.925 | - | - | 2.10 | - |
| As | 0.016 | 0.023 | 0.023 | 0.352 | - | 1.44 | 22.00 | - |
| Ni | 0.015 | 0.196 | 0.075 | 1.421 | 0.404 | 5.00 | 94.73 | 2.06 |
| Mn | 0.201 | 0.310 | - | 3.183 | 0.115 | - | 15.84 | 0.37 |
| Zn | 0.149 | 0.901 | 0.009 | 14.879 | 9.290 | 0.06 | 99.86 | 10.31 |
| Ba | 0.243 | 323.6 | 0.101 | 20.179 | 69.123 | 0.42 | 83.04 | 0.21 |
| Cu | 0.042 | 0.353 | 0.063 | 3.972 | 1.313 | 1.50 | 94.57 | 3.72 |
| Sr | 0.052 | 6.264 | - | 2.631 | 2.709 | - | 50.60 | 0.43 |

Comparing the released content of meals from studied PP MPs samples with the current EU regulations for drinking water quality, it can be observed that most of obtained values are well below limits. The only exception is Al in the leachate of PP-MPs/56 sample, which concentration exceeds set upper limits for drinking water by more than 3-fold, indicating potential toxic effects [66,67]. It should be noted that current EU Drinking Water Directive does not include mandatory limits for Ca and Mg [66], although it has been discussed that minimum limits of these essential metals are necessary for maintaining a healthy state of organisms, e.g. for 70-kg organism recommended total daily intake is 20-80 mg $L^{-1}$ of each metal [68]. However, such limits for Ca and Mg have been established in 10 out of 28 EU

countries, ranging from 100-270 mg $L^{-1}$ and 30-125 mg $L^{-1}$, respectively. WHO Guidelines for drinking water quality correlated the limits for Ca and Mg with the total hardness (100-300 mg $L^{-1}$), which can result in corrosion of water pipes and high soap consumption [69]. Another metal that has not been considered in EU Directive [53] is Sr, which detected concentrations in European waters range from 0.001 to 13.6 mg $L^{-1}$. On the other hand, U.S. Environmental Protection Agency (EPA) currently defines a non-regulatory health-based screening level of Sr; the total daily intake is 4 mg $L^{-1}$ [70]. It is known that Sr has a beneficial impact on bone growth, caries prevention and is used in the treatment methods of osteoporosis, however, high concentrations might be correlated with cardiovascular problems. The synergistic effect of Ca and Sr is important for bone health, where low Ca and high Sr may induce dysplasia and epiphysis. Competitive adsorption between Ca and Sr can induce bone deformity; therefore, the importance of Sr/Ca ratio in water is crucial [71]. Besides, the maximum limit of Ti in drinking water is also not regulated, although its various and large applications (e.g., in cosmetics, pigments, aerospace, marine, and medical) suggests its widespread presence, thus requesting regulation. The data for acute toxicity of $TiO_2$ (as a most common form of Ti) suggests that intake could be quite high ($LD_{50}$ (oral, rat) > 10000 mg $kg^{-1}$) [72]. However, detailed chronic tests should be performed to confirm Ti harmless.

Based on the above presented characterization and leaching tests, it can be concluded that altered structure of the polymer molecule due to aging results in the weakening of PP properties, enabling easier release of metals, present as residues of polymerization catalysts and added colorants.

### *3.3. Environmental aspects of MPs leachate*

The toxicity of studied leachates obtained from PP-MPs/0, PP-MPs/56, and PP-MPs/A samples was tested on three model organisms: *VF*, *DM*, and *PS*, determining the maximal

inhibition toward test organism, as well as the overall toxicity over common toxicity parameter "*effective concentration*" (EC) at different levels: $EC_{50}$, $EC_{20}$ and $EC_{10}$, determining the concentration of toxic substances causing adverse effects to 50, 20 and 10% of population, respectively. The results for the maximal inhibition toward three test organisms caused by PP-MPs/0, PP-MPs/56, and PP-MPs/A leachates are presented in Fig. 8(A). In the case of *VF*, the inhibition of bioluminescence after the 15-min exposure did not exceed 50% for all studied PP MPs samples. However, in the case of *DM* and *PS*, leachates showed more adverse effects resulting in inhibitions significantly higher than 50% in all cases (Fig. 8(A)). Based on TOC analysis, where <1 mg C $L^{-1}$ in cases of all leachates were detected, as well as the fact that monomers (propylene) used to produce PP are not hazardous [73], the observed toxic effects in our study can be assigned to released metals. The results indicate that higher concentrations of the mixtures of metals leached, recorded for PP-MPs/A and particularly PP-MPs/56 (Table 3), significantly inhibit the mobility of the crustaceans as well as the growth of the algal cells in comparison to the bacterial photoluminescence. Based on the obtained inhibition, it can be concluded that *DM* is particularly sensitive to mixtures of metals in leachates, albeit present at low concentrations. Total concentrations of metals in leachates amount 0.98, 128.81 and 13.48 μM in cases of PP-MPs/0, PP-MPs/56, and PP-MPs/A, respectively. Namely, the toxicity toward *DM* exceeded 70% inhibition even for PP-MPs/0 sample possessing rather low concentrations of metals in the leachate (Table 3). Fig. 8(B) presents values of standard toxicity parameters, $EC_{50}$ and its variants $EC_{20}$ and $EC_{10}$, toward *VF* for the leachates of the studied PP MPs. As can be seen, only PP-MPs/A leachate exhibited $EC_{50}$ value, amounting 48.7%, while $EC_{20}$ and $EC_{10}$ values were determined for all studied leachates, amounting between 22.7-33.8% and 14.5-25.4%, respectively. As mentioned above, all detected metals in leachates, with the exception of Al in PP-MPs/56, are present in concentrations that are below regulatory limits (if set by the current EU legislation).

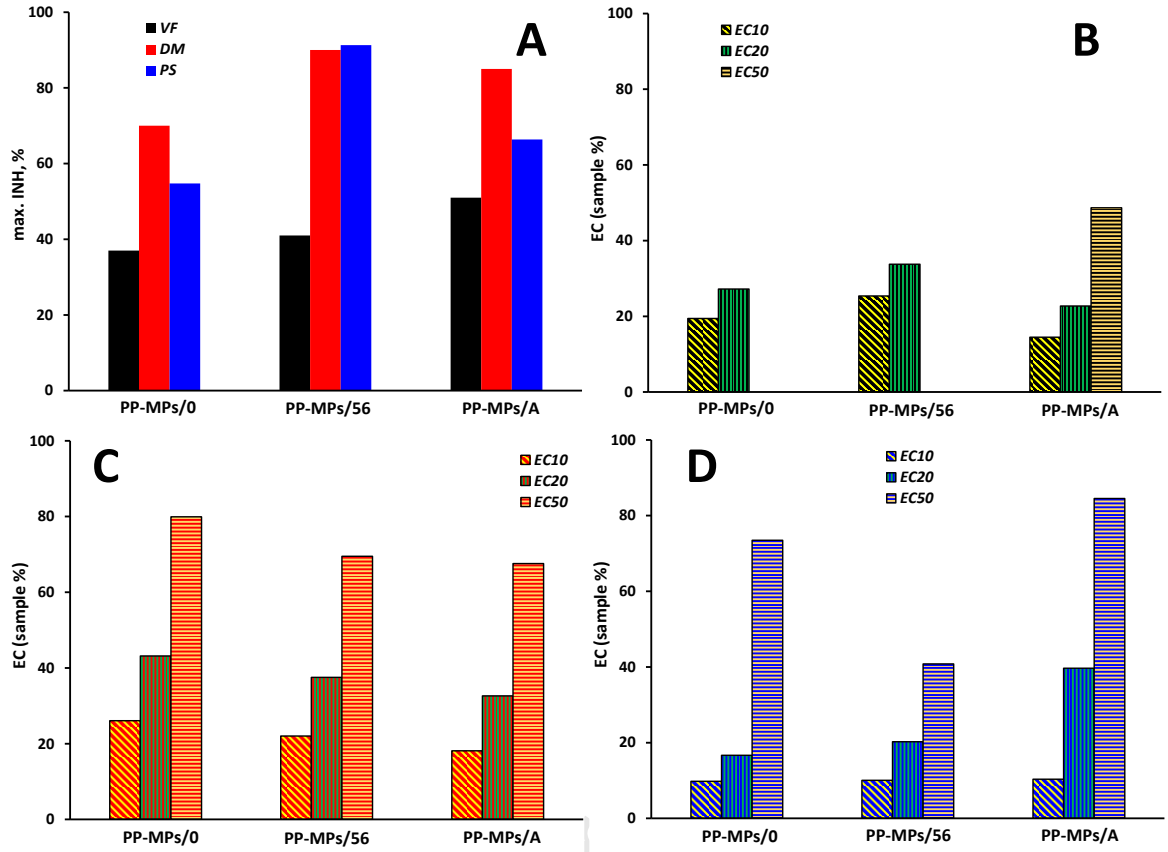


**Figure 8**. Maximal inhibitions of *Vibrio fischeri* (VF), *Daphnia magna* (DM), and *Pseudokirchneriella subcapitata* (PS) determined in leachates from PP-MPs/0, PP-MPs/56, and PP-MPs/A (A), and effective concentrations in case of leachates from PP-MPs/0, PP-MPs/56, and PP-MPs/A determined after 15 min of exposure to *VF* (B), after 48 h of exposure to *DM* (C), and 72 h of exposure to *PS* (D)

The leachate obtained from PP-MPs/56 sample, exhibiting 41% maximal bacterial luminescence inhibition (Fig. 8(A)), contains Al present in concentration far over set limits but also rather high concentrations of Fe and Zn, as well as not insignificant levels of Pb, Mn, V, Cu and Sr (Table 3), which all can contribute to the overall toxicity. Literature findings reveal that Al does not cause high acute toxic effects to *VF*; $LD_{50}$ (24 h exposure) amounts 219.6 mg $L^{-1}$ [24]. However, the tendency for bioaccumulation in human organisms is documented, which in the long run represents the inevitable cause of serious health issues such as cardiac fibrosis

as well as myocytes degeneration [25]. Furthermore, Zn and Cu in similar doses to our data (Table 3) were found to be highly toxic to *VF*; LOEC (*L*owest *O*bserved *E*ffect *C*oncentration) reported in the literature range between 10.0–40.2 and 3.39–6.78 μg $L^{-1}$, respectively [26]. The negative influence of Fe restriction on *VF* is well-documented in literature; it causes slower growth and induction of luminescence. Therefore, Fe presence has important positive effects on immune cell function and immune activation, so relatively high concentrations in our case should not represent a problem for bacterial growth [74]. Toxic effects of Pb and V on *VF* were documented in concentrations between 1-6 mg $L^{-1}$ and 0.07-1.1 mg $L^{-1}$, respectively [75,76]. However, those are much higher than those recorded in our study for any of the leachates (Table 3). Although PP-MPs/56 and PP-MPs/A leachates exhibited rather high concentrations of Ca and Mg, it seems that those did not cause significant negative effects toward VF. Considering *VF* is marine bacteria, most probably such conditions would serve as a nutrient, thus enhancing bacterial metabolism processes and growth. Namely, average marine salinity (NaCl) is 35 g $L^{-1}$, along with 1.3 g $L^{-1}$ of Mg, which is above concentrations found in our PP-MPs/56 and PP-MPs/A leachates.

Different toxicity trend is noticed when DM is used as test organism (Fig. 8(C)). $EC_{50}$ values were determined for all three leachates. As can be seen, PP-MPs/56 and PP-MPs/A exhibited similar $EC_{50}$ values (~70%), which is not surprising since much higher amounts of leached metals were present in their leachates than that of pristine sample, possessing $EC_{50}$ of 80% (Table 3, Fig. 8(C)). As opposite to bacteria, freshwater crustaceans have less tolerance to the increased amounts of Na, Ca, K, and Mg. However, since freshwater used in toxicity tests contained $MgSO_4$, $CaCl_2$, KCl, and $NaHCO_3$, the influence of these metals leached from PP-MPs cannot be fully elucidated. The distinction in sensitivity of tested organisms can also be noticed for the toxicity testing of Sr. Literature study revealed that among five different freshwater organisms, *DM* showed the lowest $IC_{50}$ ("*inhibitory concentration*") after 21-day

exposure (40 mg $L^{-1}$), while the next one was *PS* (over 72-hours exposure) resulting with $IC_{25}$ of 53 mg $L^{-1}$. It was also reported that exposure of *DM* to 2 mg $L^{-1}$ of Sr caused a decrease in fertility and an increase in mortality in subsequent generations (>90%) [77]. Such findings support the hypothesis that long-term exposure to metals enhances toxic effects. Besides, PP-MPs/56 and PP-MPs/A leachates contained much higher concentrations of Fe and Zn than PP-MPs/0 leachate (Table 3). Zn is categorized as highly toxic to aquatic organisms; $EC_{50}$ reported for *DM* is 70 μg $L^{-1}$ [78]. Daily exposure of *DM* to Fe (620 μg $L^{-1}$) resulted in low acute toxic effects due to the rapid oxidation of $Fe^{2+}$ into $Fe^{3+}$, followed by its precipitation forming larger particles. Furthermore, 8-day exposure revealed a decrease in the viability of the offspring, due to the strong accumulation of Fe in the digestive tract. The tested water samples in the study of van Anholt et al. [79], besides Fe, also contained Al (270 μg $L^{-1}$), Cd (0.1 μg $L^{-1}$), Cu (4 μg $L^{-1}$), and Pb (2.5 μg $L^{-1}$), which influenced the overall toxicity as well as bioaccumulation in the organism. Hence, the similarity to our samples is quite large, providing plausible explanation for toxic effects observed in our study for leachates PP-MPs/A and particularly PP-MPs/56 (Fig. 8(C)).

The performed toxicity test on algae (*PS*) is probably the most appropriate for the studied samples since it was run for 72 hours, much longer than in the other two toxicity tests, thus the effects of leached metals might be more evident. The results are presented in Fig. 8(D). It can be observed that $EC_{10}$ values are very similar for all three leachate samples. $EC_{20}$ values follow increasing order PP-MPs/0 < PP-MPs/56 < PP-MPs/A, while the lowest $EC_{50}$ value, i.e. the highest toxicity, was recorded for PP-MPs/56 sample, which was expected due to the highest amount of leached metals (Table 3). Microalgae is often used for water remediation of metals such as Fe or Al. For example, *Chlorella sp*. showed significant resistance to Fe compared to other tested microalgae, but *Chlamydomonas sp*. showed strong bioaccumulation; 900 μg $g^{-1}$ of initial 12 mg $L^{-1}$ ferric nitrate was accumulated [80]. It was also reported that growth

inhibition of *Scenedesmus sp*. and *Chlorella sp.* occurs at Al concentrations of 4 μmol $L^{-1}$, which is much lower than in our case [81,82]. The algal medium used for the dilution of the toxicant mainly consists of $KH_2PO_4$, $CaCl_2$, $MgSO_4$ and NaCl, therefore the influence of leached Na, K, Ca and Mg in our leachates can most probably be neglected. It was reported that toxic effect of heavy metals (Cd, Pb and Cu appearing at 25, 250, and 10 μg $L^{-1}$, respectively) may be related to the production of reactive oxygen species (ROS); algae respond by the induction of several antioxidants and enzymes such as superoxide dismutase, catalase, glutathione peroxidase and ascorbate peroxidase, and with the synthesis of low molecular weight compounds such as carotenoids and glutathione [83]. Since the physiological causes leading toward algal growth inhibition are not completely understood, the reduction of chlorophyll content and modification of mitochondrial membrane potential of *PS* has been investigated. Hence, the loss of membrane integrity was observed at 1.9 μmol $L^{-1}$ of Cd, 41 μmol $L^{-1}$ of Cr (VI), 1.3 μmol $L^{-1}$ of Cu, and 2.5 μmol $L^{-1}$ of Zn [84] which are in fact concentrations very close to those present in PP-MPs/56 leachate in our study (Table 3) providing plausible explanation for the toxicity observed (Fig. 8(D)). It should be noted that Ba and Sr inhibit and cause malformations in algal cells (*Micrasterias sp*.) as tend to crystallize at concentrations of 250 μmol $L^{-1}$ [85], which should not be completely ignored in our case. Besides, mutual synergistic effects of metals must also be considered since it is well-known how mixtures can show increased toxicity in comparison to the individual components [21].

In order to assess biodegradability, a well-known biodegradable compound (glucose, 10 mg $L^{-1}$), part of $BOD_5$ standard [38], was intentionally added to leachates containing metals and negligible content of released organics from MPs. Due to the fact that pure leachates contain negligible concentration of organics (<1 mg C $L^{-1}$), the addition of organic substrate was necessary in order to obtain $BOD_5$ value. Namely, COD values of leachates (without glucose) were determined based on the ability of metals to undergo chemical oxidation reactions, thus

yielding $O_2$ consumption recorded by applied COD test. However, $BOD_5$ values of pure leachates can not be determined due to the fact that metals are not biodegradable [86]. Glucose, as a readily biodegradable compound poses $BOD_5$/COD ratio of 0.68 (Fig. 9.), which is close to the literature reported value [38]. However, presence of metals in various concentration in our leachates altered such value depending on the leachate source.

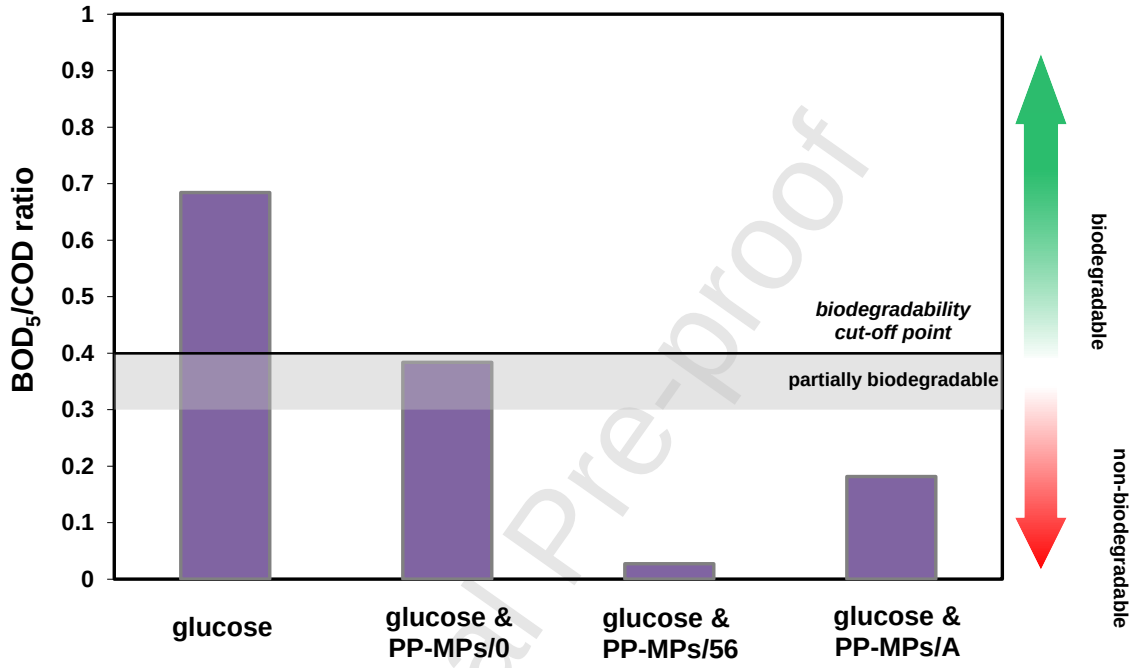


**Figure 9**. Biodegradability of glucose influenced by studied leachates.

As can be seen, glucose biodegradability was lowered to 0.38 by the presence of leached metals from PP-MPs/0 sample (Fig. 9.). However, such value is still close to the biodegradable limit, which amounts 0.4 [87]. Biodegradability of glucose was inhibited to the higher extent by PP-MPs/56 leachate ($BOD_5$/COD=0.03) (Fig. 9), which contains much higher concentration of metals comparing to PP-MPs/0 leachate (Table 3). Similar, but less emphasized effect is also observed in the case of PP-MPs/A leachate ($BOD_5$/COD=0.18) (Fig. 9). Although most of the metals in leachates were present in trace concentrations (as discussed above for toxicity results), even at such low concentrations there are four potential patterns of metals actions toward biodegradability of organics: (i) inhibition increases with increasing metal concentration; (ii)

low concentrations stimulate, while high concentrations inhibit; (iii) high concentrations inhibit less; and (iv) mild inhibition remains constant [27]. According to the results presented in Fig. 9 and Table 3., the first scenario is responsible for the effects observed in our study. According to the literature findings [27,86], individual metals contributing to the lowering glucose biodegradability are Al, present in rather high concentrations in both PP-MPs/A and particularly PP-MPs/56 leachates, as well as metals present in much lower concentrations such as Zn, Ba, Cu, Sr, Mn, and even Pb and Cr. Although Fe is present in rather high concentrations in PP-MPs/56 leachate, it has the lowest influence on the biodegradability among detected metals, and even may stimulate it at certain conditions [27,86]. It should be noted that such findings are important to understand biodegradation processes in the presence of MPs occurring in nature, but also in water treatment plants (during secondary cycle).

## 4. CONCLUSIONS

Based on the obtained results it can be concluded that photo-aging of PP would promote MPs generation, particularly fractions with rather small particles. The reason for such effect can be associated with the fact that photo-aged PP has damaged structure, with increased C.I. and newly formed carbonyl and unsaturated ketone groups. The aged PP samples also showed decrease in crystallinity, and severe changes in surface morphology. All these changes were reflected in increased brittleness, and thus in the formation of MPs of small sizes. The leaching tests showed more intense releasing of metals, mostly in trace concentrations, from photo-aged and waste packaging PP than from the pristine analogue. Such behavior in the case of photo-aged PP can be closely correlated with the damaged structure due to aging process, allowing easier release of metals present in the structure into aquatic environment. On the other hand, higher concentrations in leachate from waste packaging PP are due to trace metals present in the pigments used for the coloration. However, the concentrations of all detected metals in

leachates are below limits set by current legislation, except for Al. The highest toxic effects were observed again in the case of photo-aged and waste packaging PP, while the most sensitive organism among tested to the leached metals was shown to be the freshwater crustacean *Daphnia magna*. In the case of all three tested organisms, maximal inhibition (%) did not exceed 90%. Biodegradation of leachates followed the same trend, where PP-MPs/A and particularly PP-MPs/56 leachates strongly inhibited glucose biodegradability due to present metals such Al, Mn, Zn, Ba, Cu, Sr, and even Pb and Cr, although present in rather low concentrations.

**ACKNOWLEDGMENT**

We would like to acknowledge the financial support by the Croatian Science Foundation under the projects *Microplastics in water; fate and behavior and removal*, ***ReMiCRO*** (IP-2020-02-6033).

**REFERENCES**

1. Statista. https://www.statista.com/statistics/1103529/global-polypropyleneproduction/. Accessed: 25 January 2023
2. OECD (2022), Global Plastics Outlook: Policy Scenarios to 2060, OECD Publishing, Paris, https://doi.org/10.1787/aa1edf33-en.
3. Dimassi, S. N.; Hahladakis, J. N.; Daly Yahia, M. N.; Ahmad, M. I.; Sayadi, S.; Al-Ghouti, M. A. Degradation-fragmentation of marine plastic waste and their environmental implications: A critical review. *Arab. J. Chem*. **2022**, *15*, 104262. DOI: https://doi.org/10.1016/j.arabjc.2022.104262

4. Guo, Y.; Xia, X.; Ruan, J.; Wang, Y.; Zhang, J.; LeBlanc, G. A.; An, L. Ignored microplastic sources from plastic bottle recycling. *Sci. Total Environ.* **2022**, *838*, 156038. DOI: https://doi.org/10.1016/j.scitotenv.2022.156038

5. Suzuki, G.; Uchida, N.; Huu Tuyen, L.; Tanaka, K.; Matsukami, H.; Kunisue, T.; Takahashi, S.; Viet, P. H.; Kuramochi, H.; Osako, M. Mechanical recycling of plastic waste as a point source of microplastic pollution. *Environ. Pollut.* **2022,** *303*, 119114. DOI: https://doi.org/10.1016/j.envpol.2022.119114

6. Hahladakis, J.N.; Velis, C.A.; Weber, R.; Iacovidou, E.; Purnell, P. An overview of chemical additives present in plastics: Migration, release, fate and environmental impact during their use, disposal and recycling. *J. Hazard. Mater*. **2018,** *344*, 179–199. DOI: https://doi.org/10.1016/j.jhazmat.2017.10.014

7. Murphy, J., 2001. Additives for Plastics Handbook, Second edition. Elsevier, Amsterdam.

8. European Commission, Directive (EU) 2019/904 of the European Parliament and of the Council of 5 June 2019 on the reduction of the impact of certain plastic products on the environment. *Off. J. Eur. Union* **2019**, *L155*, 1-19.

9. Commission Regulation (EU) No 10/2011 of 14 January 2011 on plastic materials and articles intended to come into contact with food, *Off. J. Eur. Union* **2011**, *L12*, 1-89.

10. Guzzonato, A.; Puype, F.; Harrad, S.J. Evidence of bad recycling practices: BFRs in children's toys and food-contact articles. *Environ. Sci. Process. Impacts* **2017.** *19*, 956–963. DOI: https://doi.org/10.1039/C7EM00160F

11. Eriksen, M.K.; Pivnenko, K.; Olsson, M.E.; Astrup, T.F. Contamination in plastic recycling: Influence of metals on the quality of reprocessed plastic. *Waste Manage*. **2018.** *79*, 595–606. DOI: https://doi.org/10.1016/j.wasman.2018.08.007

12. Peng, L.; Fu, D.; Qi, H.; Lan, C.; Yu, H.; Ge, C. Micro and nano plastics in marine environment: source, distribution and threats—a review. *Sci. Total Environ*. **2020.** *698*, 134254. DOI: https://doi.org/10.1016/j.scitotenv.2019.134254

13. De Sá, L.C.; Oliveira, M.; Ribeiro, F.; Rocha, T. L.; Futter, M. N. Studies of the effects of microplastics on aquatic organisms: what do we know and where should we focus our efforts in the future? *Sci. Total Environ.* **2018.** *645*, 1029–1039. DOI: https://doi.org/10.1016/j.scitotenv.2018.07.207

14. Peacock, A. J.; Calhoun, A. Polymer Chemistry Properties and Applications, Hanser Publishers, Munich, Hanser Gardner Publications, Cincinnati, 2006.

15. Akoueson, F.; Paul-Pont, I.; Tallec, K.; Huvet, A.; Doyen, P.; Dehaut, A.; Duflos, G. Additives in polypropylene and polylactic acid food packaging: Chemical analysis and bioassays provide complementary tools for risk assessment. *Sci. Total Environ.* **2022,** *857*, 159318. DOI: https://doi.org/10.1016/j.scitotenv.2022.159318

16. Zimmermann, L.; Bartosova, Z.; Braun, K.; Oehlmann, J.; Völker, C.; Wagner, M. Plastic Products Leach Chemicals That Induce In Vitro Toxicity under Realistic Use Conditions. *Environ. Sci. Technol*. **2021,** *55*, 11814−11823. https://doi.org/10.1021/acs.est.1c01103

17. Cverenkárová, K.; Valachovičová, M.; Mackuľak, T.; Žemlička, L.; Bírošová, L. Microplastics in the Food Chain. *Life* **2021.** *11*, 1349. https://doi.org/10.3390/life11121349

18. Smith, E. C.; Turner, A. Mobilisation kinetics of Br, Cd, Cr, Hg, Pb and Sb in microplastics exposed to simulated, dietary-adapted digestive conditions of seabirds. *Sci. Total Environ*. **2022,** *733*, 138802. https://doi.org/10.1016/j.scitotenv.2020.138802

19. Biale, G.; La Nasa, J.; Mattonai, M.; Corti, A.; Castelvetro, V.; Modugno, F. Seeping plastics: Potentially harmful molecular fragments leaching out from microplastics during

accelerated ageing in seawater, *Water Res.* **2022**, 219, 118521. https://doi.org/10.1016/j.watres.2022.118521

20. Menicagli, V.; Balestri, E.; Biale, G.; Corti, A.; La Nasa, J.; Modugno, F.; Castelvetro, V.; Lardicci, C. Leached degradation products from beached microplastics: A potential threat to coastal dune plants, *Chemosphere* 2022, **303**, 135287. https://doi.org/10.1016/j.chemosphere.2022.135287
21. Wu, X.; Cobbina, S. J.; Mao, G.; Xu, H.; Zhang, Z.; Yang, L. A review of toxicity and mechanisms of individual and mixturesof heavy metals in the environment. *Environ. Sci. Pollut. Res.* **2016**, *23*, 8244–8259. https://doi.org/10.1007/s11356-016-6333-x
22. Riyazuddin, R.; Nisha, N.; Ejaz, B.; Khan, M. I. R.; Kumar, M.; Ramteke, P. W.; Gupta, R. A Comprehensive Review on the Heavy Metal Toxicity and Sequestration in Plants. *Biomolecules* **2022**, *12*(1), 43. https://doi.org/10.3390/biom12010043
23. Vardhan, K. H.; Kumar, P. S.; Panda, R. C. A review on heavy metal pollution, toxicity and remedial measures: Current trends and future perspectives. *J. Mol. Liquids* **2019**, *290*, 111197. https://doi.org/10.1016/j.molliq.2019.111197
24. Strigul, N.; Vaccari, L.; Galdun, C.; Wazne, M.; Liu, X.; Christodoulatos, C.; Jasinkiewicz, K. Acute toxicity of boron, titanium dioxide, and aluminum nanoparticles to *Daphnia magna* and *Vibrio fischeri*. *Desalination*, **2009**, *248*, 771-782. https://doi.org/10.1016/j.desal.2009.01.013
25. Novaes, R. D.; Mouro, V.G.S.; Gonçalves, R.V.; Mendonça, A.A.S.; Santos, E.C.; Fialho, M.C.Q., Machado-Neves, M. Aluminum: A potentially toxic metal with dose-dependent effects on cardiac bioaccumulation, mineral distribution, DNA oxidation and microstructural remodeling. *Environ. Pollut.* **2018**, *242*, 814-826. https://doi.org/10.1016/j.envpol.2018.07.034

26. Hsieh, C.Y.; Tsai, M.H.; Ryan, D.K.; Pancorbo, O.C. Toxicity of the 13 priority pollutant metals to *Vibrio fisheri* in the Microtox chronic toxicity test. *Sci. Total Environ*. **2004**, *320*, 37-50. https://doi.org/10.1016/S0048-9697(03)00451-0

27. Feng, J.-R.; Ni, H.-G. Effects of heavy metals and metalloids on the biodegradation of organic contaminants. *Environ. Res.* **2024**, *246*, 118069. https://doi.org/10.1016/j.envres.2023.118069

28. Sandrin, T.R.; Maier, R.M. Impact of metals on the biodegradation of organic pollutants. *Environ. Health Perspect*. **2003**, *111*, 1093-1101. https://doi.org/10.1289/ehp.5840

29. Almond, J.; Sugumaar, P.; Wenzel, M.N.; Hill, G.; Wallis, C. Determination of the carbonyl index of polyethylene and polypropylene using specified area under band methodology with ATR-FTIR spectroscopy, *e-Polymers* **2020.** *20* 369–381. https://doi.org/10.1515/epoly-2020-0041

30. Brandon, J.; Goldstein, M.; Ohman, M. D. Long-term aging and degradation of microplastic particles: Comparing in situ oceanic and experimental weathering patterns, *Mar. Pollut. Bull.* **2016.** *110*, 299–308. https://doi.org/10.1016/j.marpolbul.2016.06.048

31. Lanyi, F.J.; Wenzke, N.; Kaschta, J.; Schubert, D.W. On the Determination of the Enthalpy of Fusion of α-Crystalline Isotactic Polypropylene Using Differential Scanning Calorimetry, X Ray Diffraction, and Fourier-Transform Infrared Spectroscopy: An Old Story Revisited. *Adv. Eng. Mater.* **2019.** *22*, 1900796. https://doi.org/10.1002/adem.201900796

32. EN 14429:2015, Characterization of waste - Leaching behaviour test - Influence of pH on leaching with initial acid/base addition.

33. EN 13130-1:2004, Materials and articles in contact with foodstuffs - Plastics substances subject to limitation - Part 1: Guide to test methods for the specific migration of substances

from plastics to foods and food simulants and the determination of substances in plastics and the selection of conditions of exposure to food simulants.

34. Commission Regulation (EU) 2020/1245, of 2 September 2020, amending and correcting Regulation (EU) No 10/2011 on plastic materials and articles intended to, come into contact with food.
35. International Organisation for Standardisation. (2007). Water quality — Determination of the inhibitory effect of water samples on the light emission of Vibrio fischeri (Luminescent bacteria test) — Part 3: Method using freeze-dried bacteria (ISO Standard No. 11348-3:2007), https://www.iso.org/standard/40518.html
36. International Organisation for Standardisation. (2012). Water quality — Determination of the inhibition of the mobility of Daphnia magna Straus (Cladocera, Crustacea) — Acute toxicity test (ISO Standard No. 6341:2012), https://www.iso.org/standard/54614.html
37. International Organisation for Standardisation. (2012). Water quality — Fresh water algal growth inhibition test with unicellular green algae (ISO Standard No. 8692:2012), https://www.iso.org/standard/54150.html
38. Pasco, N.; Baronian, K.; Jeffries C., Hay J. Biochemical mediator demand – a novel rapid alternative for measuring biochemical oxygen demand. *Appl. Microbiol. Biotechnol.* **2000**, *53*, 613–618. https://doi.org/10.1007/s002530051666
39. Tochácek, J.; Vrátnícková, Z. Polymer life-time prediction: The role of temperature in UV accelerated ageing of polypropylene and its copolymers, *Polym. Test.* **2014**, *36*, 82-87. https://doi.org/10.1016/j.polymertesting.2014.03.019
40. Frigione, M.; Rodríguez-Prieto, A. Can Accelerated Aging Procedures Predict the Long Term Behavior of Polymers Exposed to Different Environments?, *Polymers* **2021**, *13: 2688*, 1-18. https://doi.org/10.3390/polym13162688

41. Simunovic, M.; Kusic, H.; Koprivanac, N.; Loncaric Bozic, A. Treatment of simulated industrial wastewater by photo-Fenton process: Part II. The development of mechanistic model, *Chem. Eng. J.* **2011**, *173*, 280-289. https://doi.org/10.1016/j.cej.2010.09.030

42. Fang, J.; Zhang, L.; Sutton, D.; Wang, X.; Lin, T. Needleless Melt-Electrospinning of Polypropylene Nanofibres, *J. Nanomater*. **2012**. 2012, 1–9. https://doi.org/10.1155/2012/382639

43. Prabowo, I.; Nur Pratama, J.; Chalid, M. The effect of modified ijuk fibers to crystallinity of polypropylene composite, *Mater. Sci. Eng*., **2017.** *223*, 012020. 10.1088/1757-899X/223/1/012020

44. Maier, C.; Calafut, T. Polypropylene: the definitive user's guide and databook, William Andrew, 1998. 3-7.

45. Wu, H.; Zhao, Y.; Dong, X.; Su, L., Wang, K.; Wang, D. Probing into the microstructural evolution of isotactic polypropylene during photo-oxidation degradation. *Polym. Degrad. Stab.* **2021.** *183*, 109434. https://doi.org/10.1016/j.polymdegradstab.2020.109434

46. Song, Y.K.; Hong, S. H.; Jang, m.; Han, G. M.; Jung, S. W.; Shim, W. J. Combined Effects of UV Exposure Duration and Mechanical Abrasion on Microplastic Fragmentation by Polymer Type. *Environ. Sci. Technol*. **2017**. *51*, 4368−4376. https://doi.org/10.1021/acs.est.6b06155

47. Gijsman, P. Polymer Stabilization, In: Kutz, M., Handbook of Environmental Degradation of Materials, William Andrew, 2018. 369-395.

48. Rouillon, C.; Bussiere, P.-O.; Desnoux, E.; Collin, S.; Vial, C.; Therias, S.; Gardette, J.-L. Is carbonyl index a quantitative probe to monitor polypropylene photodegradation? *Polym. Degrad. Stab.* **2016,** *128*, 200-208. https://doi.org/10.1016/j.polymdegradstab.2015.12.011

49. Cavalcanti, R.S. de F.B.; Rabello, M.S. The Effect of Red Pigment and Photo Stabilizers on the Photo Degradation of Polypropylene Films. *Mater. Res*. **2019.** *22*, 1-8. https://doi.org/10.1590/1980-5373-MR-2018-0708

50. Rtimi, S., Pulgarin, C., Sanjinesb, R., Kiwi, J., Novel FeOx–polyethylene transparent films: synthesis and mechanism of surface regeneration. *RSC Adv.* **2015.** *5*, 80203-80211. https://doi.org/10.1039/C5RA14503A

51. Tziourrou, P., Vakros, J., Karapanagioti, H.K. Using diffuse reflectance spectroscopy (DRS) technique for studying biofilm formation on LDPE and PET surfaces: laboratory and field experiments. *Environ. Sci. Pollut. Res.* **2020.** 27, 12055–12064. https://doi.org/10.1007/s11356-020-07729-0.

52. Su, W. F., Characterization of Polymer, In: Principles of Polymer Design and Synthesis, Springer, Berlin, Germany, 2013, 89–110.

53. Głuszewski, W., Application of DRS to study the processes of postradiation degradation of polypropylene, Institute of nuclear chemistry and technology http://www.ichtj.waw.pl/ichtj/, Warszawa, Poland, 2021.

54. Aslanzadeh, S.; Haghighat Kish, M. Photo-oxidation of polypropylene fibers exposed to short wavelength UV radiations. *Fibers Polym.* **2010.**. 11, 710–718. https://doi.org/10.1007/s12221-010-0710-8

55. Uheida, A.; Mejía, H.G.; Abdel-Rehim, M.; Hamd, W.; Dutta, J. Visible light photocatalytic degradation of polypropylene microplastics in a continuous water flow system, *J. Hazard. Mater.* **2021.** *406*, 124299. https://doi.org/10.1016/j.jhazmat.2020.124299

56. Scoti, M.; De Stefano, F.; Di Girolamo, R.; Malafronte, A.; Talarico, G.; De Rosa, C. Crystallization Behavior and Properties of Propylene/4-Methyl-1-pentene Copolymers

from a Metallocene Catalyst, *Macromolecules* **2023**, *56*, 1446–1460. https://doi.org/10.1021/acs.macromol.2c02232

57. Rabello Tand, M.S.; Whit, J.R. Crystallization and melting behaviour of photodegraded polypropylene– Il. Re-crystallization of degraded molecules. *Polyme*r, **1997.** 38, 6389–639. https://doi.org/10.1016/S0032-3861(97)00213-9
58. Jabarin, S.A.; Lofgren, E.A. Photooxidative effects on properties and structure of high-density polyethylene, *J. Appl. Polym. Sci.* **1994.** *53*, 411-423. https://doi.org/10.1002/app.1994.070530404
59. Stark, N.M.; Matuana L.M.; Clemons, C.M. Effect of processing method on surface and weathering characteristics of wood–flour/HDPE composites. *J. Appl. Polym. Sci*. **2004.** *93*, 1021-1030. https://doi.org/10.1002/app.20529
60. Liu, P.; Zhan, X.; Wu, X.; Li, J.; Wang, H.; Gao, S. Effect of weathering on environmental behavior of microplastics: Properties, sorption and potential risks, *Chemosphere*, **2019.** *242*, 125193. https://doi.org/10.1016/j.chemosphere.2019.125193
61. Nunes, R.W.; Martin, J.R.; Johnson, J.F. Influence of molecular weight and molecular weight distribution on mechanical properties of polymers. *Polym. Eng. Sci*. **1982**. *22*, 205–228. https://doi.org/10.1002/pen.760220402
62. Chang, M.; Liu, X.; Nelson, P. J.; Munzing, G. R.; Gegan, T. A.; Kissin, Y. V. Ziegler–Natta catalysts for propylene polymerization: Morphology and crystal structure of a fourth-generation catalyst. *J. Catal.* 2006, *239*, 347-353. https://doi.org/10.1016/j.jcat.2006.02.009
63. Potapov, A. G. Titanium-magnesium Ziegler-Natta catalysts: new insight on the active sites precursor. *Mol. Catal.* **2017**, *432*, 155-159. https://doi.org/10.1016/j.mcat.2017.02.007

64. Chancharoenrith, S.; Kamonsatikul, C.; Namkajorn, M.; Kiatisevi, S.; Somsook, E. Iron oxide/cassava starch-supported Ziegler–Natta catalysts for in situ ethylene polymerization. *Carbohydr. Polym.* **2015**, *117*, 319-323. https://doi.org/10.1016/j.carbpol.2014.09.080

65. Turner, A.; Filella, M. Hazardous metal additives in plastics and their environmental impacts. *Environ. Int.* **2021**, *156*, 106622. https://doi.org/10.1016/j.envint.2021.106622

66. Directive (EU) 2020/2184 of the European Parliament and of the Council of 16 December 2020 on the quality of water intended for human consumption (recast) https://eur-lex.europa.eu/legal-content/EN/TXT/PDF/?uri=CELEX:32020L2184&from=EN

67. Closset, M.; Cailliau, K.; Slaby, S.; Marin, M. Effects of Aluminium Contamination on the Nervous System of Freshwater Aquatic Vertebrates: A Review. *Int. J. Mol. Sci.* **2021** 23, 31 https://doi.org/10.3390/ijms23010031

68. Kozisek, F. Regulations for calcium, magnesium or hardness in drinking water in the European Union member states. *Regul. Toxicol. Pharmacol*. **2020.** *112*, 104589. https://doi.org/10.1016/j.yrtph.2020.104589

69. WHO Guidelines for drinking-water quality, 4th edition, 2011., Geneva, Switzerland, WHO Library Cataloguing-in-Publication Dana, ISBN 978 92 4 154815 1

70. Minnesota Drinking Water Information System (MNDWIS). 2018 https://www.health.state.mn.us/communities/environment/water/docs/report2018.pdf

71. Peng, H.; Yao, F.; Xiong, S. Strontium in public drinking water and associated public health risks in Chinese cities. *Environ. Sci. Pollut. Res.* **2021.** *28*, 23048–23059. https://doi.org/10.1007/s11356-021-12378-y

72. Shammas, M.A.; Ahmad, D.; Nguyen, M.D.; Rajput, S.; Unmack, J.; Ahmad, G. Suggested safe harbor limit for titanium dioxide: an exposure level which protects

consumers from cancer incidence. *Front. Oncol*. **2015.**, *76*, 1-2. https://doi.org/10.3389/fonc.2015.00076

73. Lithner, D.; Nordensvan, I.; Dave, G. Comparative acute toxicity of leachates from plastic products made of polypropylene, polyethylene, PVC, acrylonitrile–butadiene–styrene, and epoxy to Daphnia magna. *Environ. Sci. Pollut. Res.* **2011**, *19*, 1763-1772. https://doi.org/10.1007/s11356-011-0663-5

74. Dunlap, P.V. Iron control of the *Vibrio fischeri* luminescence system in *Escherichia coli*. *Arch. Microbiol.* **1992**, *157*, 235-41. https://doi.org/10.1007/BF00245156

75. Tchounwou, P.B; Reed, L; Assessment of lead toxicity to the marine bacterium, Vibrio fischeri, and to a heterogeneous population of microorganisms derived from the Pearl River in Jackson, Mississippi, USA. *Rev. Environ. Health* **1999**, *14*, 51-61. https://doi.org/10.1515/REVEH.1999.14.2.51

76. Wilk, A, Szypulska-Koziarska, D, Wiszniewska, B. The toxicity of vanadium on gastrointestinal, urinary and reproductive system, and its influence on fertility and fetuses malformations. *Postepy Hig. Med. Dosw*. **2017**, *25*, 850-859. 10.5604/01.3001.0010.4783

77. Olkova, A. Chronic Toxicity Testing with *Daphnia magna* in Three Generations. *Environ. Eng. Manag. J.* **2022.** *78*, 31–37. https://doi.org/10.5755/j01.erem.78.1.30095

78. OECD (2005) SIDS Initial Assessment Profile on zinc metal, zinc oxide, zinc distearate, zinc chloride, zinc sulphate, trizinc bis (orthophosphate). SIDS Initial Assessment Meeting, 21, 18/10/2005 http://webnet.oecd.org/HPV/UI/handler.axd?id=9a66eb20-4489-4c7e-9711-8302cde5565b (Accessed Sep 18th 2023.)

79. van Anholt, R.D.; Spanings, F.A.; Knol, A.H.; van der Velden, J.A.; Wendelaar Bonga, S.E. Effects of iron sulfate dosage on the water flea (Daphnia magna Straus) and early development of carp (Cyprinus carpio L.). *Arch. Environ. Contam. Toxicol*. **2002**, *42*, 182-92. https://doi.org/10.1007/s00244-001-0001-X

80. Teodorovic, I.; Planojevic, I.; Knezevic, P.; Radak, S.; Nemet, I. Sensitivity of bacterial vs. acute Daphnia magna toxicity tests to metals. *Cent. Eur. J. Biol.* **2009**, *4*, 482–492. https://doi.org/10.2478/s11535-009-0048-7

81. Subramaniyam, V.; Subashchandrabose, S.R.; Thavamani, P; Chen, Z.; Krishnamurti, G.S.R.; Naidu, R.; Megharaj, M. Toxicity and bioaccumulation of iron in soil microalgae. *J. Appl. Phycol.* **2016**, *7*, 2767–2776. https://doi.org/10.1007/s10811-016-0837-0

82. Lindemann, J.; Holtkamp, E.; Herrmann, R. The impact of aluminium on green algae isolated from two hydrochemically different headwater streams, Bavaria, Germany. *Environ. Pollut.* **1990**, *1*, 61-77. https://doi.org/10.1016/0269-7491(90)90172-9

83. Hollnagel, H.C.; Pinto, E.; Morse, D.; Colepicolo, P. The Oscillation of Photosynthetic Capacity in *Lingulodinium polyedrum* is not related to differences in RuBisCo, Peridinin or Chlorophyll *a* Amounts. *Biol. Rhythm Res*. **2002**, *33*, 443-458. https://doi.org/10.1076/brhm.33.4.443.8804

84. Machado, M.D.; Lopes, A.R.; Soares, E.V. Responses of the alga *Pseudokirchneriella subcapitata* to long-term exposure to metal stress. *J. Hazard. Mater.* **2015**, *296*, 82-92. https://doi.org/10.1016/j.jhazmat.2015.04.022

85. Niedermeier, M.; Gierlinger, N.; Lütz-Meindl, U. Biomineralization of strontium and barium contributes to detoxification in the freshwater alga *Micrasterias*. *J. Plant Physiol*. **2018**, *230*, 80-91. https://doi.org/10.1016/j.jplph.2018.08.008

86. Massoud, R.; Hadiani, M. R.; Hamzehlou, P.; Khosravi-Darani, K. Bioremediation of heavy metals in food industry: Application of Saccharomyces cerevisiae. *Electron. J. Biotechnol.* **2019**, *37*, 56–60. https://doi.org/10.1016/j.ejbt.2018.11.003

87. Farre, M.J.; Franch, M.I.; Ayllon, J.A.; Peral, J.; Domenech, X. Biodegradability of treated aqueous solutions of biorecalcitrant pesticides by means of photocatalytic ozonation. *Desalination* **2007**, *211,* 22–33. https://doi.org/10.1016/j.desal.2006.02.082